Supporting Information

Treating Anisotropic Artefacts in Circular Dichroism Spectroscopy Enables Investigation of Lyotropic Liquid Crystalline Polyaspartate Solutions

Max Hirschmann,[a] Christian Merten[b] and Christina M. Thiele[a,*]

[a] Clemens-Schöpf-Institute for Organic Chemistry and Biochemistry, Technical University of Darmstadt, Alarich-Weiss-Straße 4, 64287 Darmstadt, Germany

[b] Ruhr University Bochum, Faculty of Chemistry and Biochemistry, Organic Chemistry II, Universitätsstraße 150, 44801 Bochum, Germany.

* E-Mail: cthiele@thielelab.de

Table of Contents

Cuvette Holders

Two cuvette holders were constructed

a) Optional Magnetic Field Parallel to Measurement Beam (Ring Magnets)

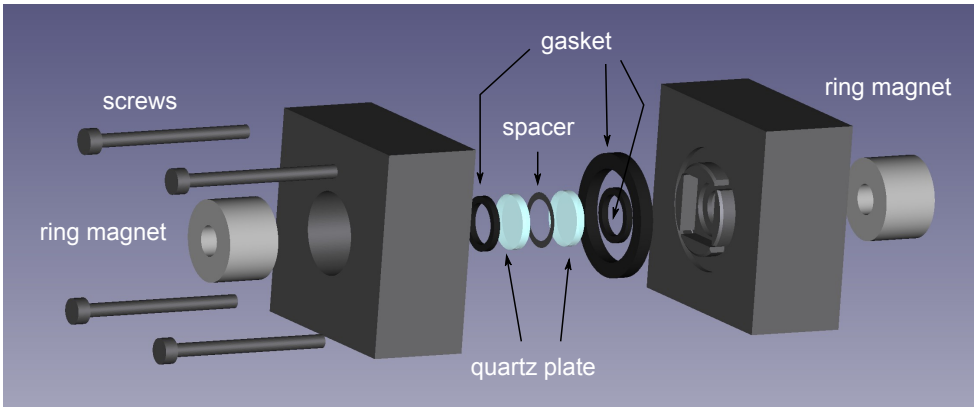

Figure S-1: Sketch of the cuvette holder allowing for an optional insertion of ring magnets that induce a magnetic field parallel to the measurement beam.

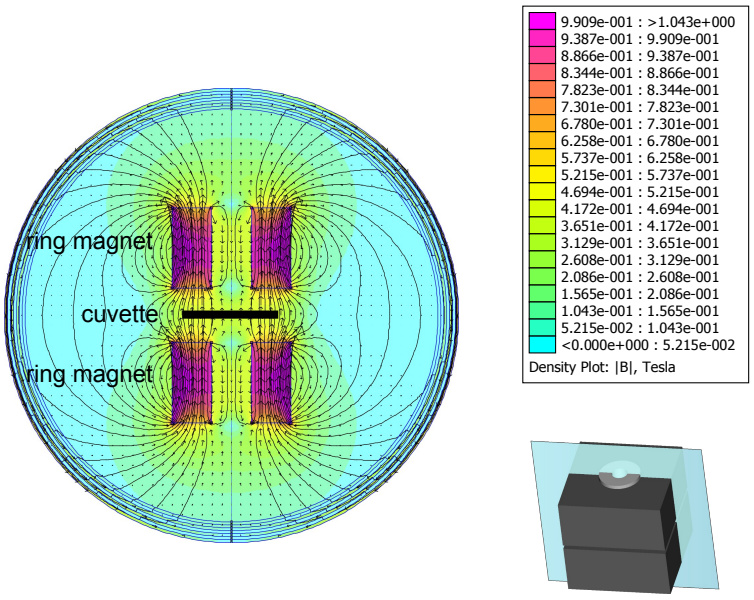

Figure S-2: Calculation of the magnetic field strength and its direction induced by the two ring magnets using the software FEMM.[1] Inside the cuvette the magnetic field is calculated to be ~0.45 T and parallel with respect to the measurement beam. For representation, the density plot originally obtained by the software FEMM was mirrored to give a full image of the setup instead of only half the image.

b) Optional Magnetic Field Perpendicular to Measurement Beam (Disc Magnets)

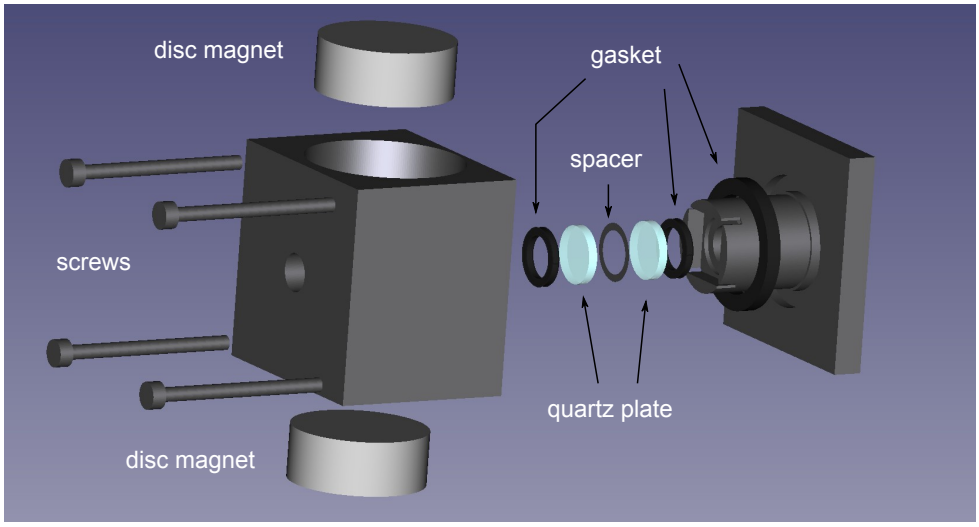

Figure S-3: Sketch of the cuvette holder allowing for an optional insertion of disc magnets that induce a magnetic field perpendicular to the measurement beam.

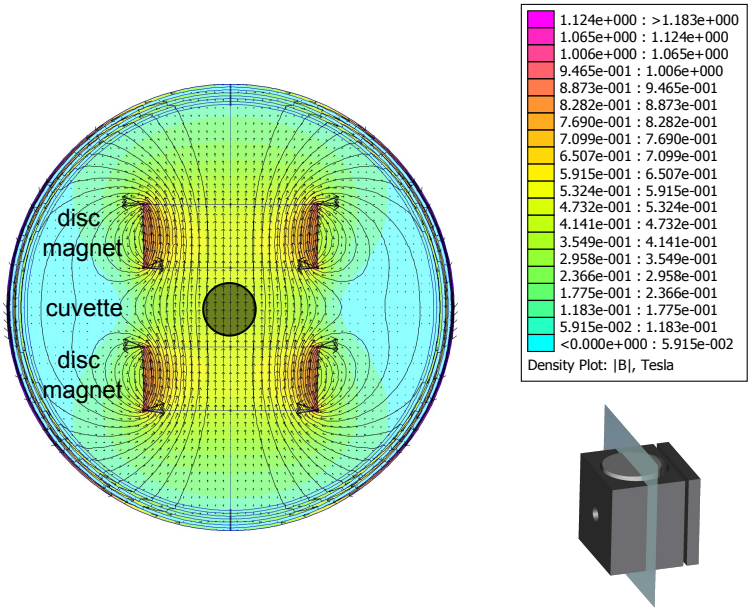

Figure S-4: Calculation of the magnetic field strength and its direction induced by the two disc magnets using the software FEMM.[1] Inside the cuvette the magnetic field is calculated to be ~0.45 T and perpendicular with respect to the measurement beam. For representation, the density plot originally obtained by the software FEMM was mirrored to give a full image of the setup instead of only half the image.

Absorbance, CD and LD Spectra

General Remarks

Background-corrected absorbance (abs), circular dichroism (CD) and linear dichroism (LD) spectra of the individual measurements (pos 1 to pos 4, sample rotations) and the average of these spectra are displayed over the entire wavelength range measured. Spectral areas for which the high tension (HT) voltage exceeds 500 V (cut-off wavelength) are greyed out.

The LLC solutions were prepared by dissolving ~20 %(w/w) (PBLA-α-*d*)$_{50\%}$-*co*-PPLA$_{50\%}$ and ~22 %(w/w) poly-β-phenethyl-L-aspartate (PPLA) in either pure TCE or AO solution (0.1 %(w/w) in TCE) in a 5 mm NMR sample tube and were homogenized by repeatedly centrifuging the sample back and forth. The equilibration of the LLC PPLA solutions, when changing the sample temperature from 280 to 310 K, was found to be significant longer compared to LLC (PBLA-α-*d*)$_{50\%}$-*co*-PPLA$_{50\%}$ solutions. Therefore, instead of measuring at both temperatures using the same sample two samples were prepared and stored overnight at 280 and 310 K, respectively, prior to measurement. The altered sign of the CD signature of AO in LLC PPLA solution at 280 and 310 K, respectively, was further verified to stem from the change in temperature and not to stem from e.g. the preparation of the sample. This was achieved by measuring the CD signal over the course of time when changing the temperature from 280 to 310 K (c.f. fig. S-15). To allow for a longer equilibration, samples measured inside a magnetic field were prepared the day before and stored at 280, 310 and 340 K, respectively, inside the cuvette holder with the magnets being inserted.

Isotropic AO Solution

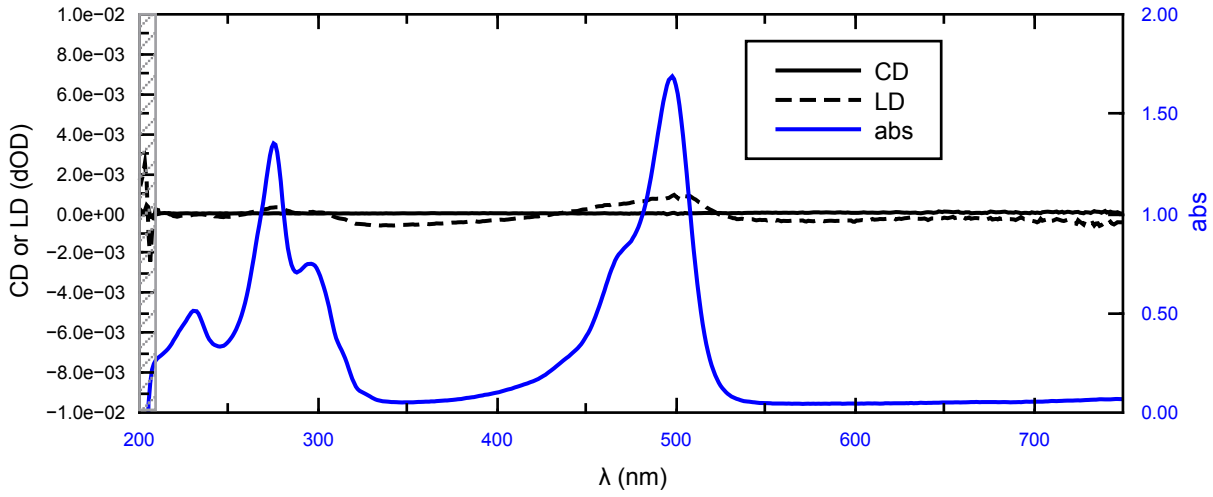

Figure S-5: Absorbance (blue), CD (black, solid) and LD (black, dashed) spectra of an isotropic AO solution (0.1 .%(w/w) in TCE).

Orange Dye, Incorporated into PET

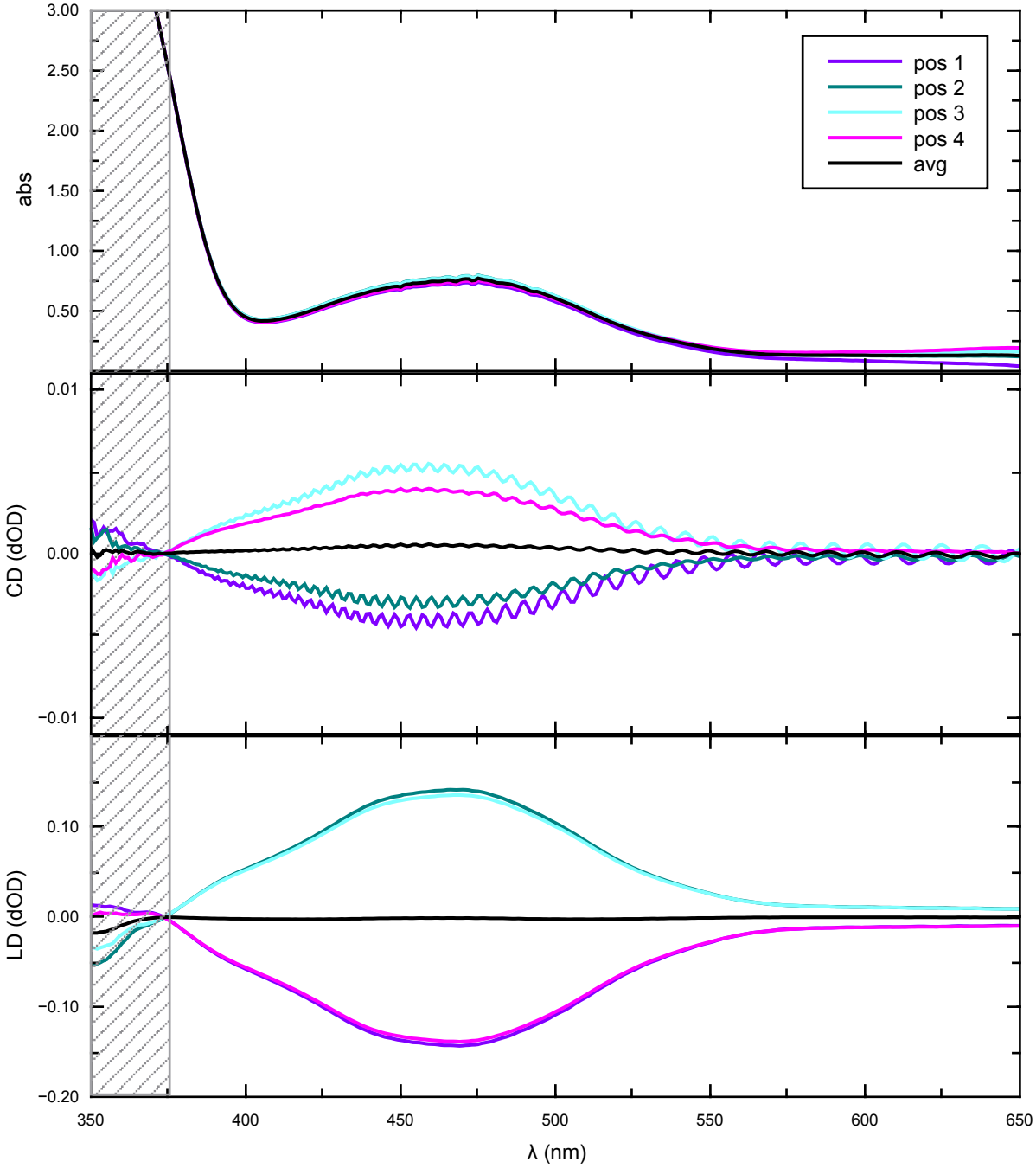

Figure S-6: Absorbance (top), CD (middle) and LD (bottom) spectra of an orange dye, incorporated into injection-moulded PET. The absorbance spectra barely change with rotation of the sample (pos 1 – pos 4) as expected if the illumination is homogenous and the sample area measured does not change with rotation. For the individual CD and LD spectra dichroism is observed due to the anisotropy of the sample that cancels out upon averaging of the four spectra.

LLC (PBLA-α-*d*)$_{50\%}$-*co*-PPLA$_{50\%}$ Solution

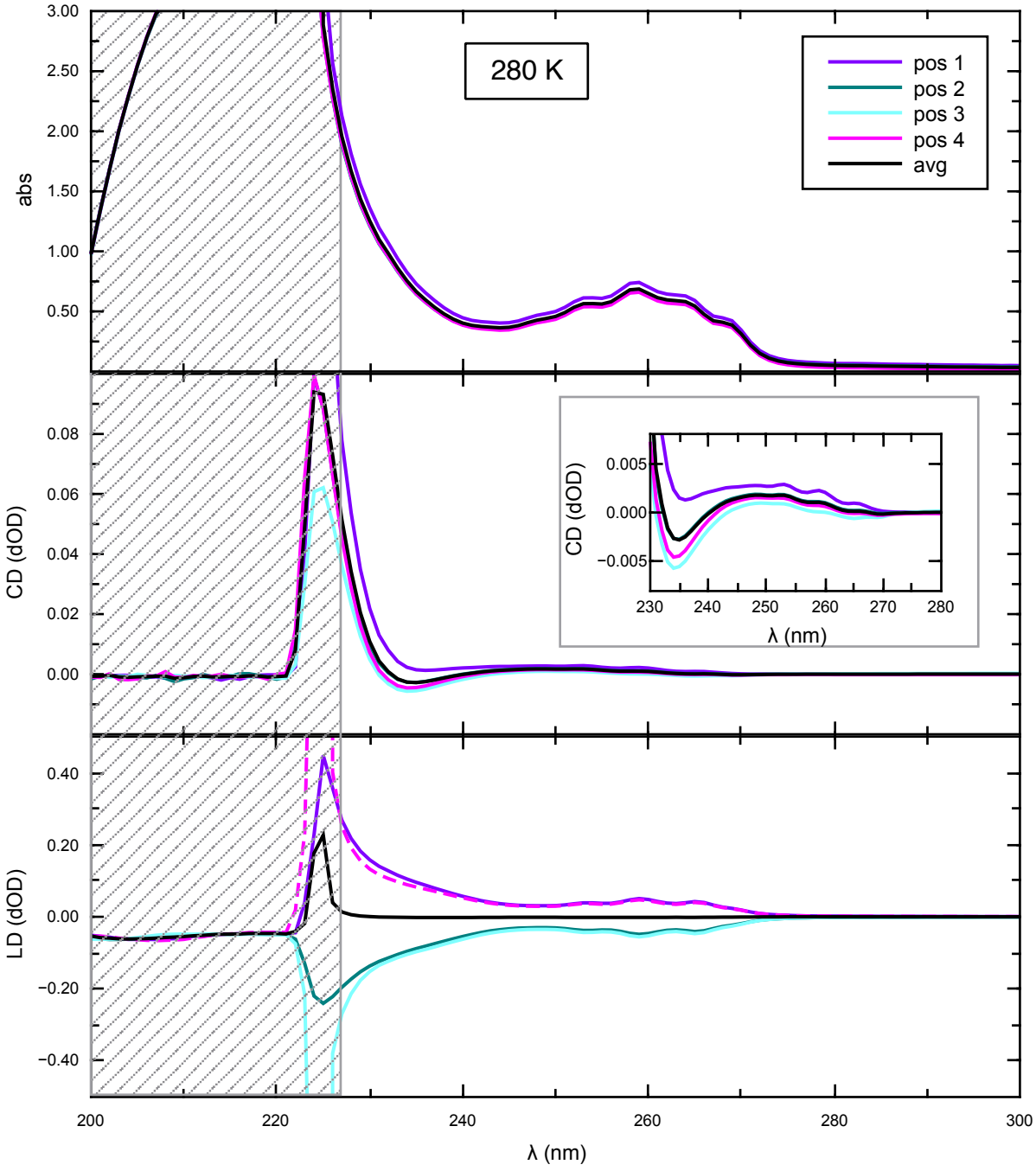

Figure S-7: Absorbance (top), CD (middle) and LD (bottom) spectra of LLC (PBLA-α-*d*)$_{50\%}$-co-PPLA$_{50\%}$ solution at 280 K.

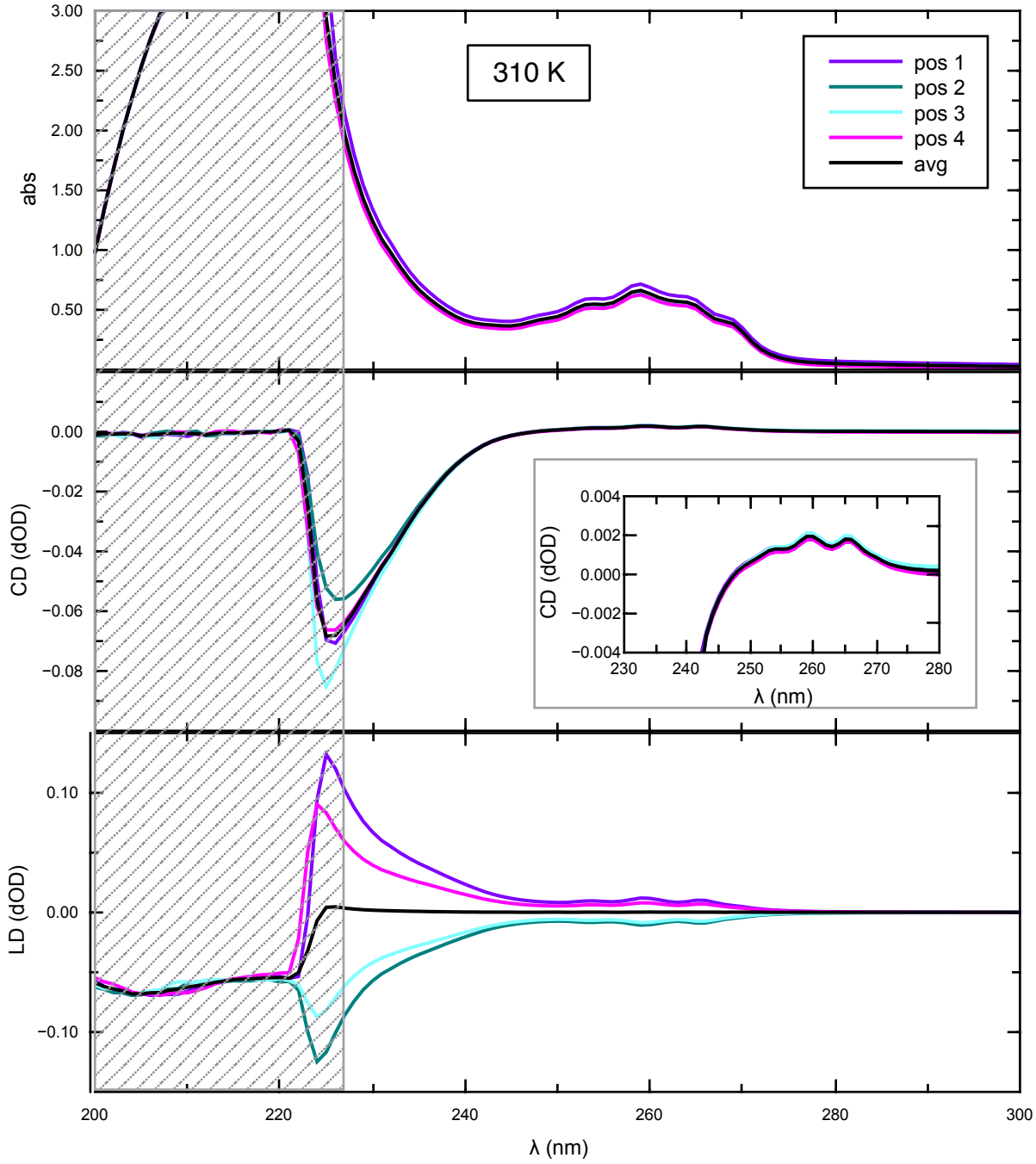

Figure S-8: Absorbance (top), CD (middle) and LD (bottom) spectra of LLC (PBLA-α-*d*)$_{50\%}$-co-PPLA$_{50\%}$ solution at 310 K.

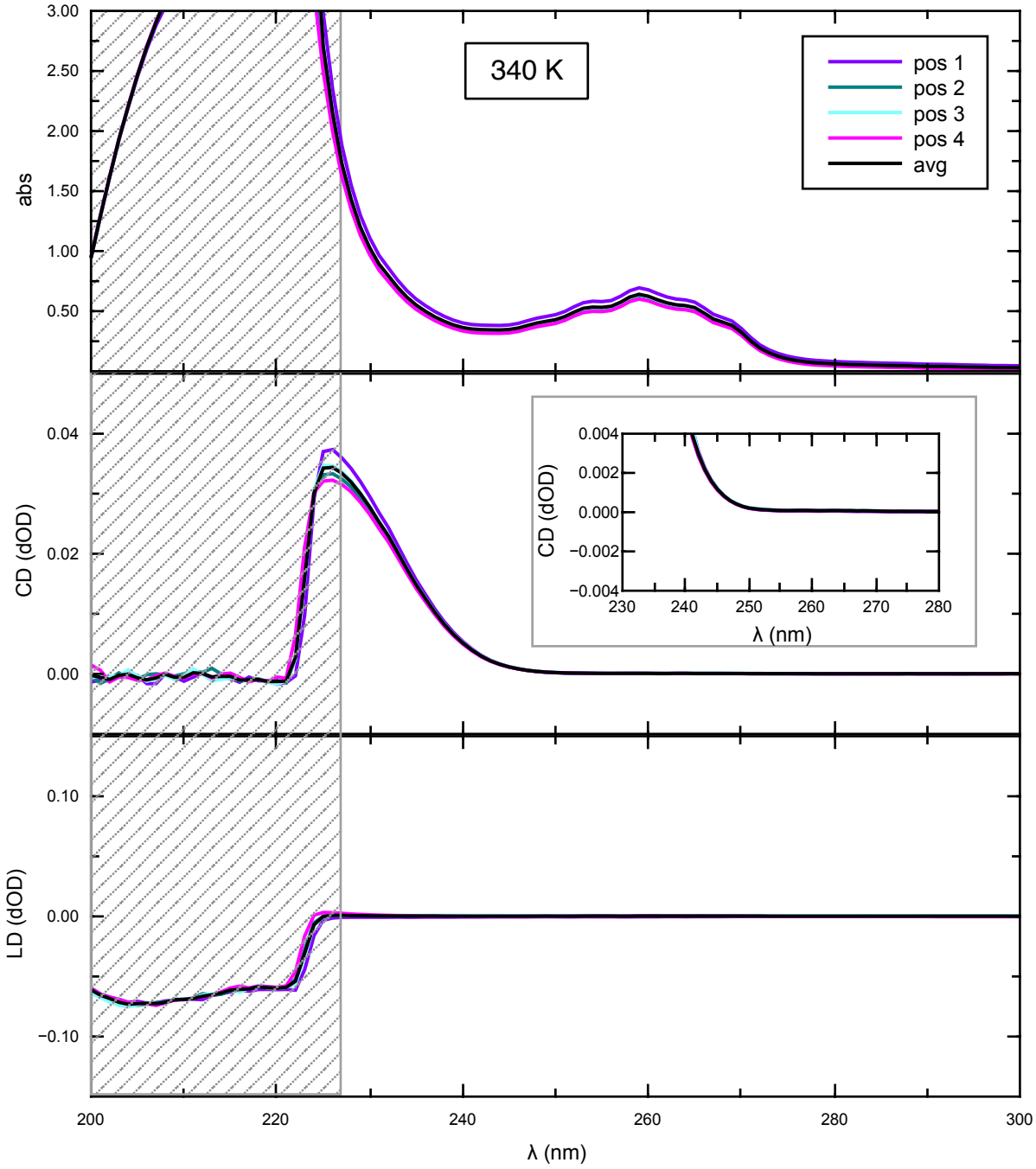

Figure S-9: Absorbance (top), CD (middle) and LD (bottom) spectra of LLC (PBLA-α-*d*)$_{50\%}$-co-PPLA$_{50\%}$ solution at 340 K.

AO in LLC (PBLA-α-*d*)$_{50\%}$-*co*-PPLA$_{50\%}$ Solution

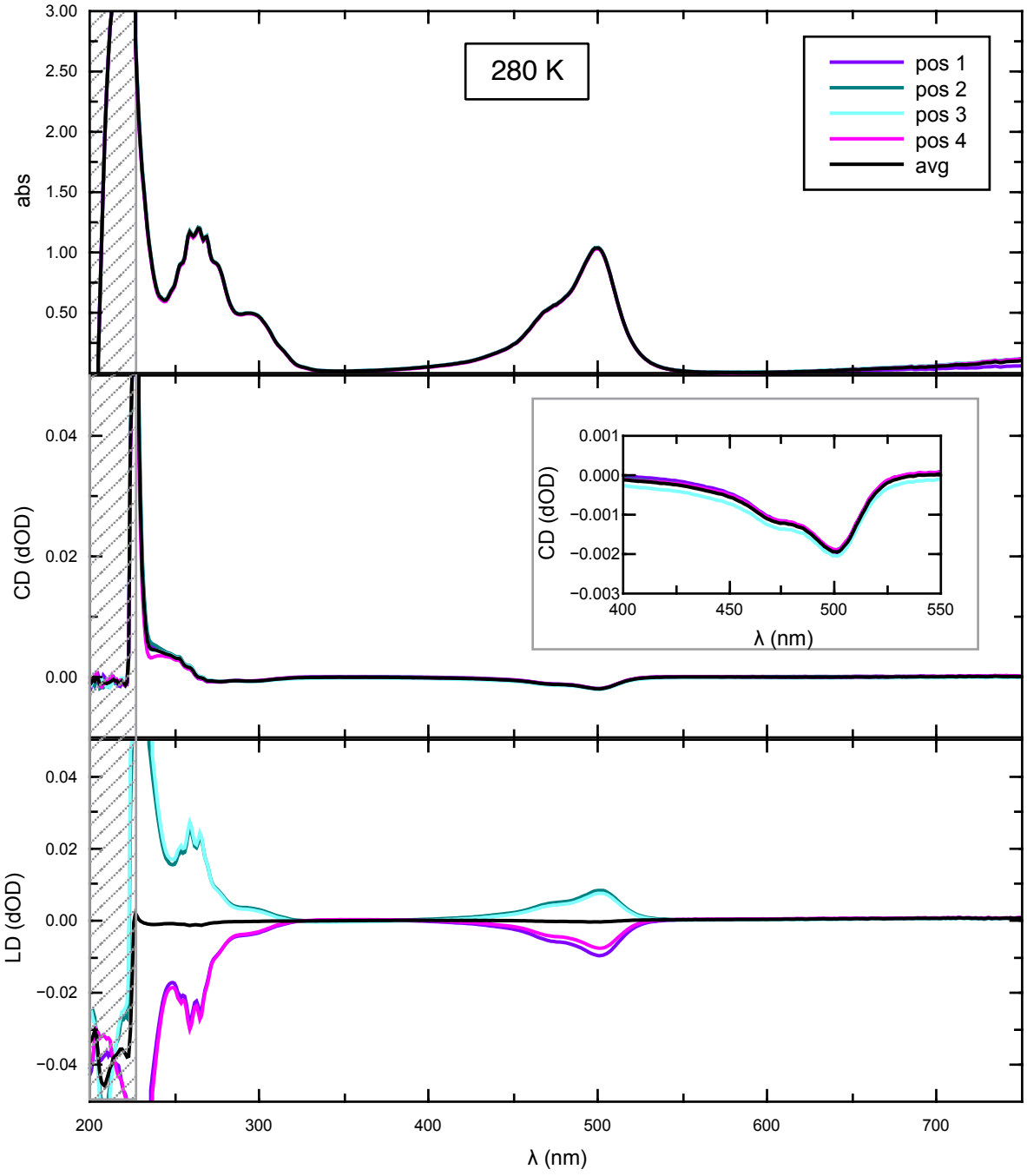

Figure S-10: Absorbance (top), CD (middle) and LD (bottom) spectra of AO in LLC (PBLA-α-*d*)$_{50\%}$-co-PPLA$_{50\%}$ solution at 280 K. Below 300 nm, the CD has contributions from the polymer (backbone and side-chain) and AO.

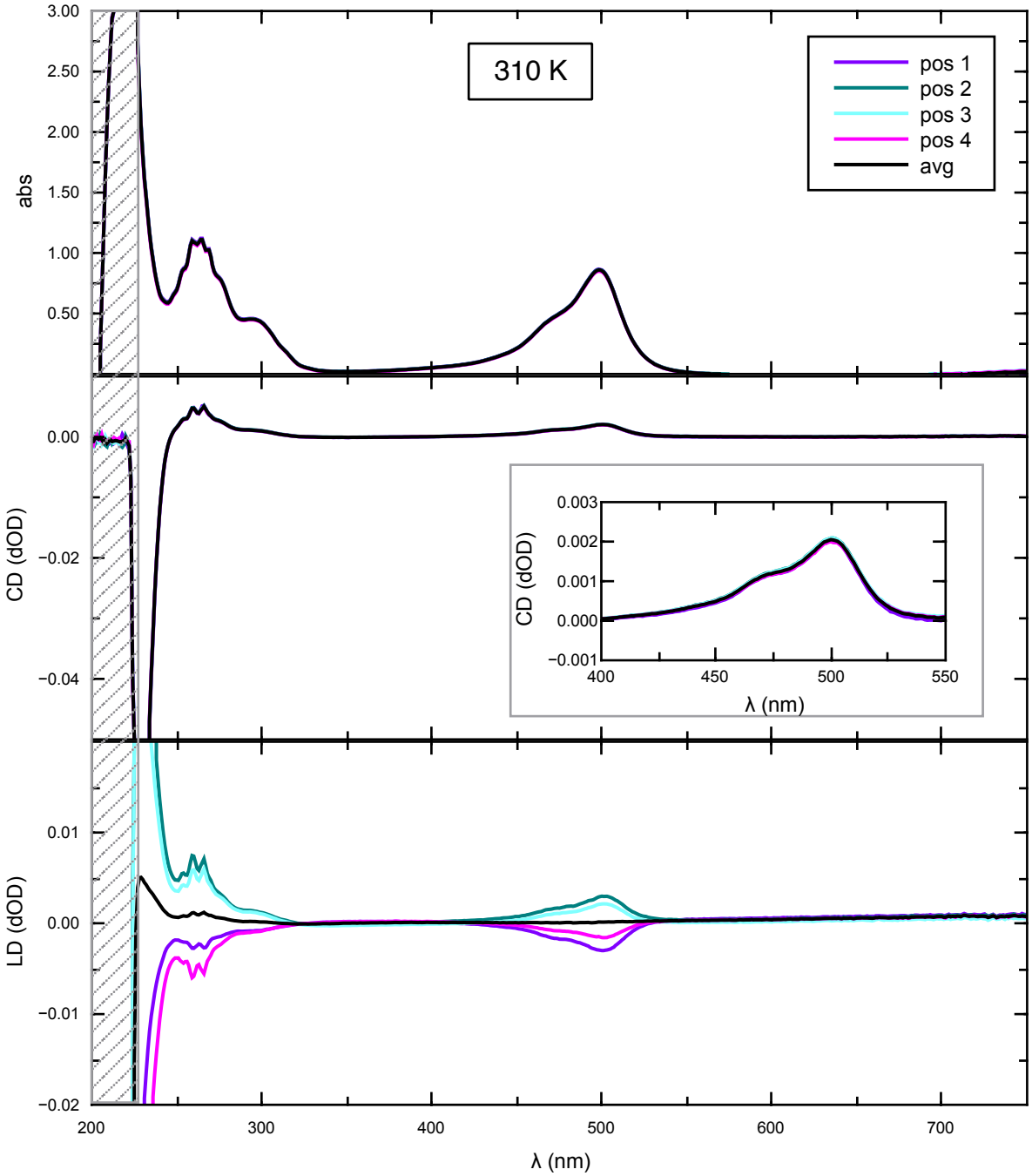

Figure S-11: Absorbance (top), CD (middle) and LD (bottom) spectra of AO in LLC (PBLA-α-*d*)$_{50\%}$-co-PPLA$_{50\%}$ solution at 310 K. Below 300 nm, the CD has contributions from the polymer (backbone and side-chain) and AO.

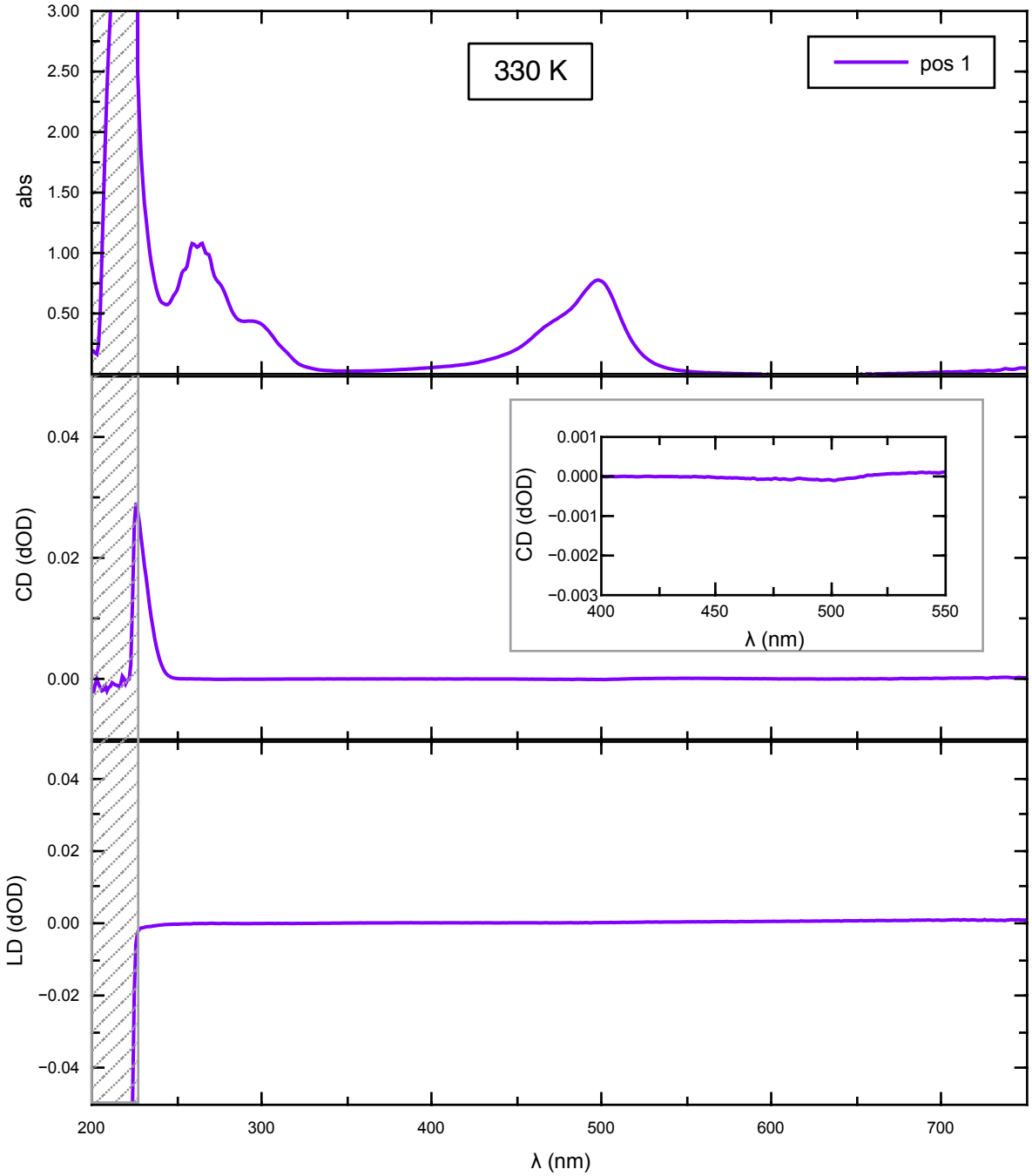

Figure S-12: Absorbance (top), CD (middle) and LD (bottom) spectra of AO in LLC (PBLA-α-*d*)$_{50\%}$-co-PPLA$_{50\%}$ solution at 330 K. The sample was measured only in position 1, no CD artefacts are observed. The absence of an induced CD of AO indicates the breakdown of the preferred cholesteric sense and, thus, the CD spectrum resembles the CD spectrum observed for pure LLC (PBLA-α-*d*)$_{50\%}$-co-PPLA$_{50\%}$ solution.

AO in LLC PPLA Solution

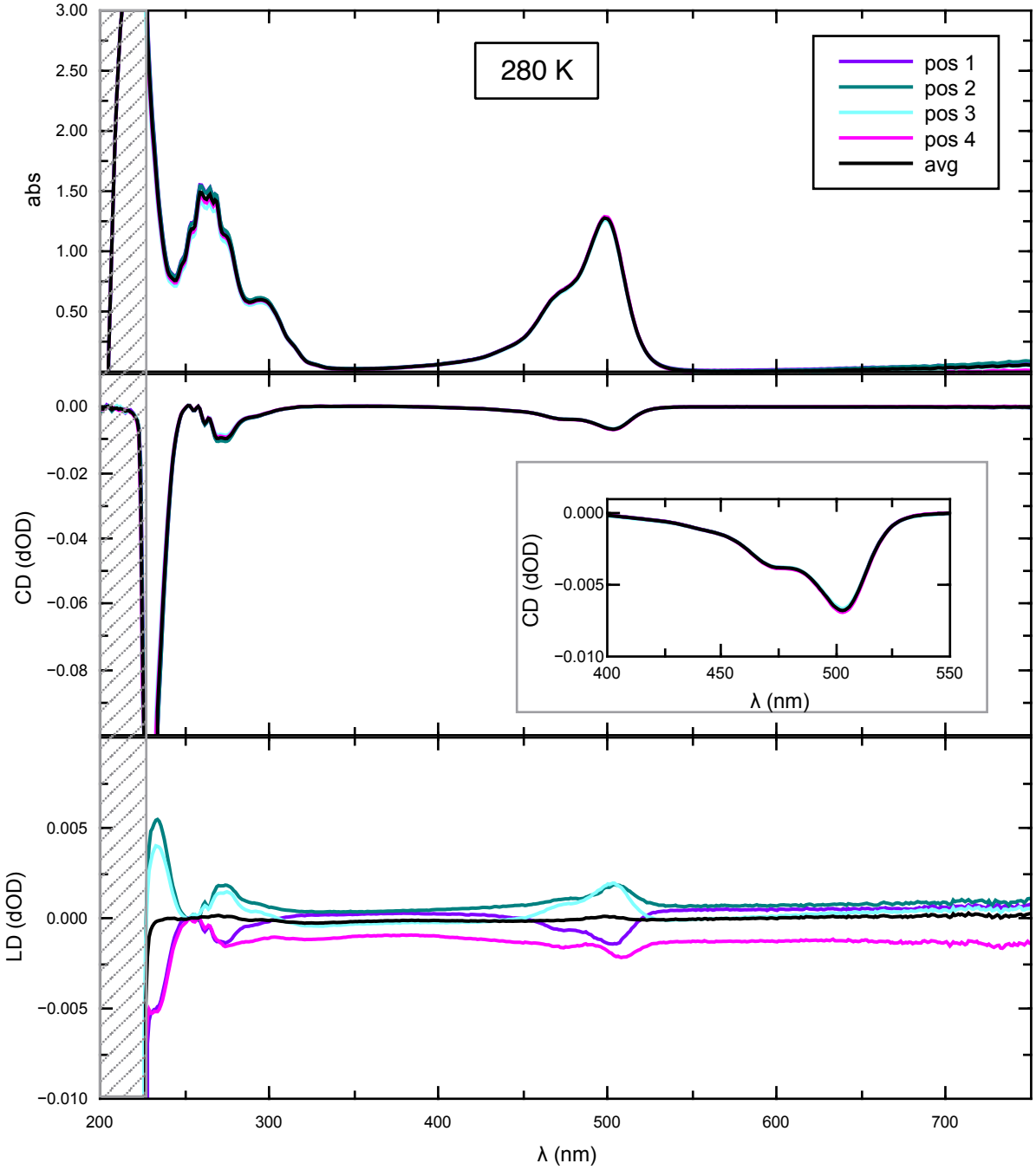

Figure S-13: Absorbance (top), CD (middle) and LD (bottom) spectra of AO in LLC PPLA solution at 280 K.

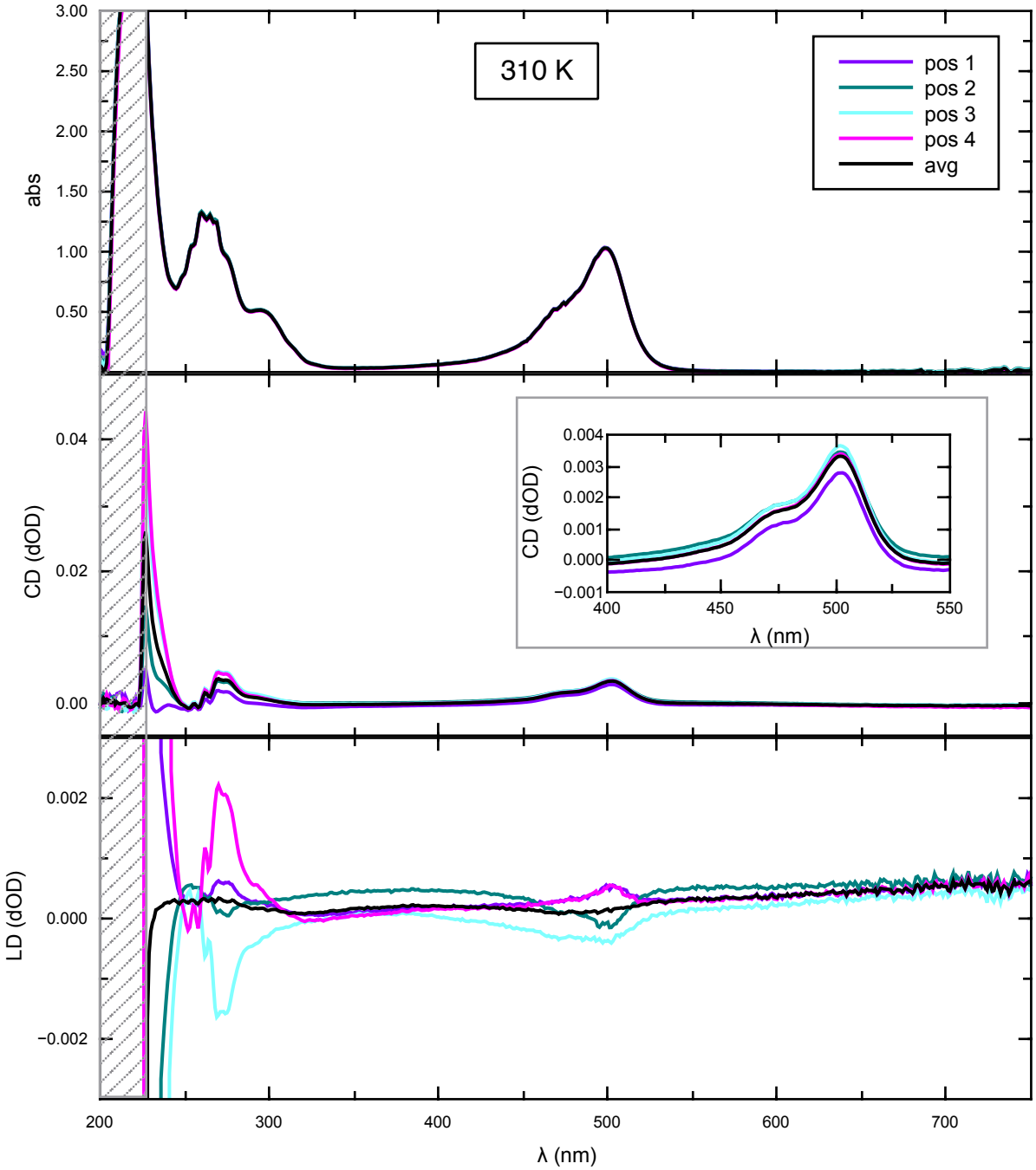

Figure S-14: Absorbance (top), CD (middle) and LD (bottom) spectra of AO in LLC PPLA solution at 310 K.

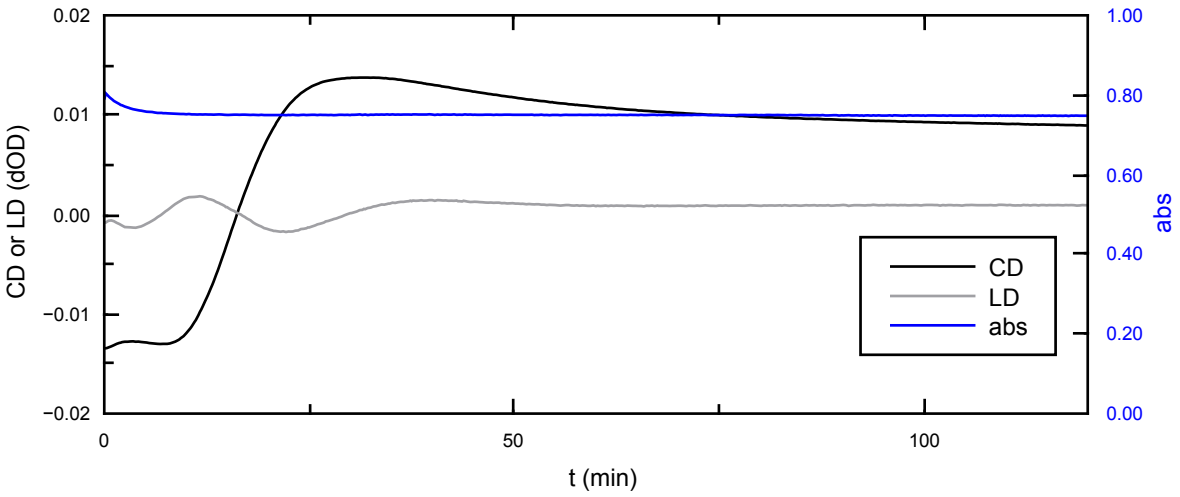

Figure S-15: Equilibration of AO in LLC PPLA solution (CD, LD and abs were measured at 500 nm) after a temperature change from 280 to 310 K. Prior to the measurement the sample was equilibrated at 280 K over night and placed inside the CD spectrometer at the same temperature (280 K). At this temperature the sample persists as a right-handed cholesteric liquid crystal (indicated by a negative CD signal). With start of the measurement (at time 0 min) the peltier element was set to 310 K. The temperature change of the peltier element and the cuvette (holder) takes a few minutes. At 310 K the sample alters the cholesteric sense from right-handed to left-handed, which results in a positive CD signal. The change of the cholesteric sense was, thus, followed over time.

LLC (PBLA-α-*d*)$_{50\%}$-*co*-PPLA$_{50\%}$ Solution Inside Magnetic Field Parallel to the Measurement Beam

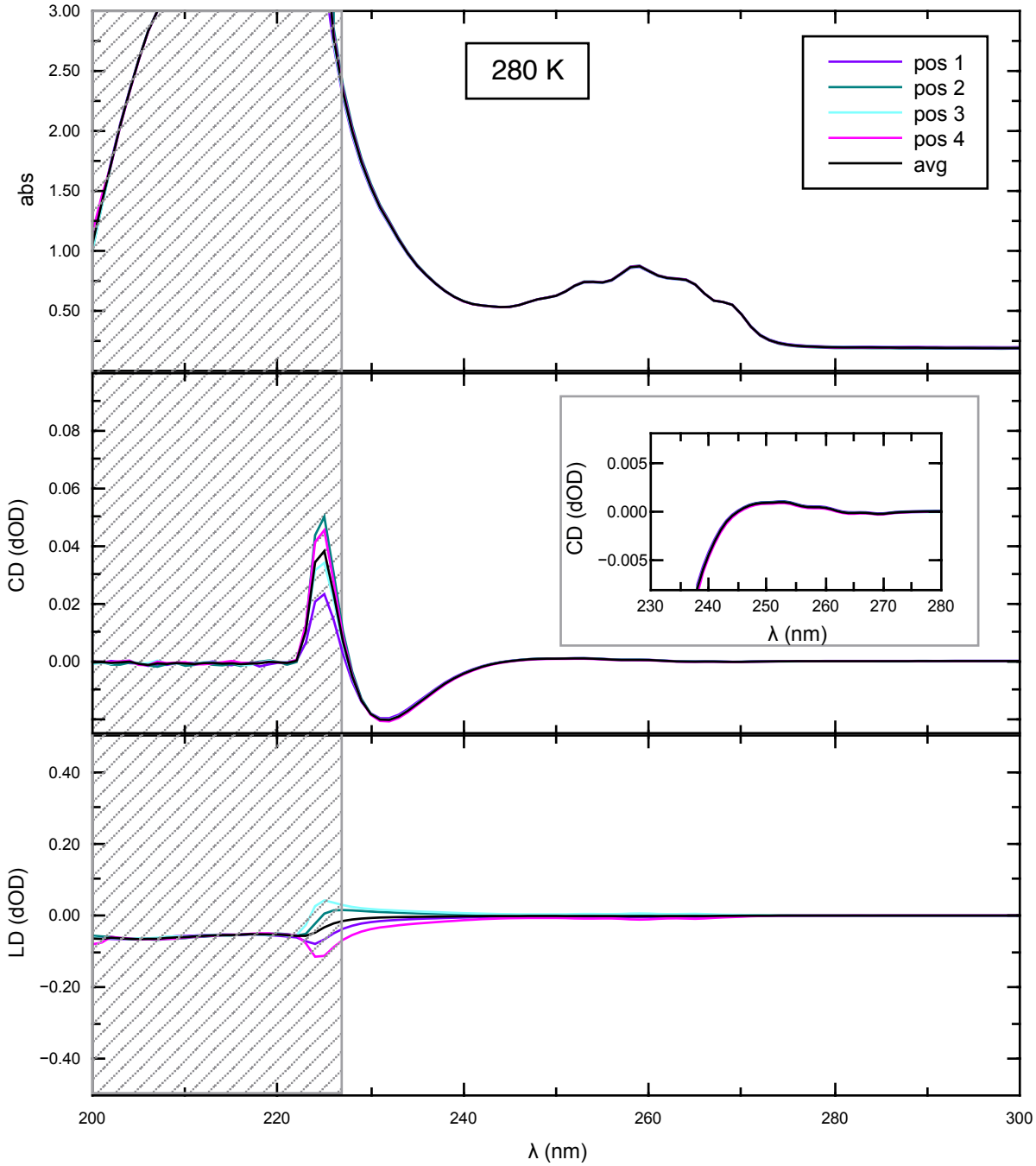

Figure S-16: Absorbance (top), CD (middle) and LD (bottom) spectra of LLC (PBLA-α-*d*)$_{50\%}$-co-PPLA$_{50\%}$ solution inside a parallelly aligned magnetic field with respect to the measurement beam at 280 K.

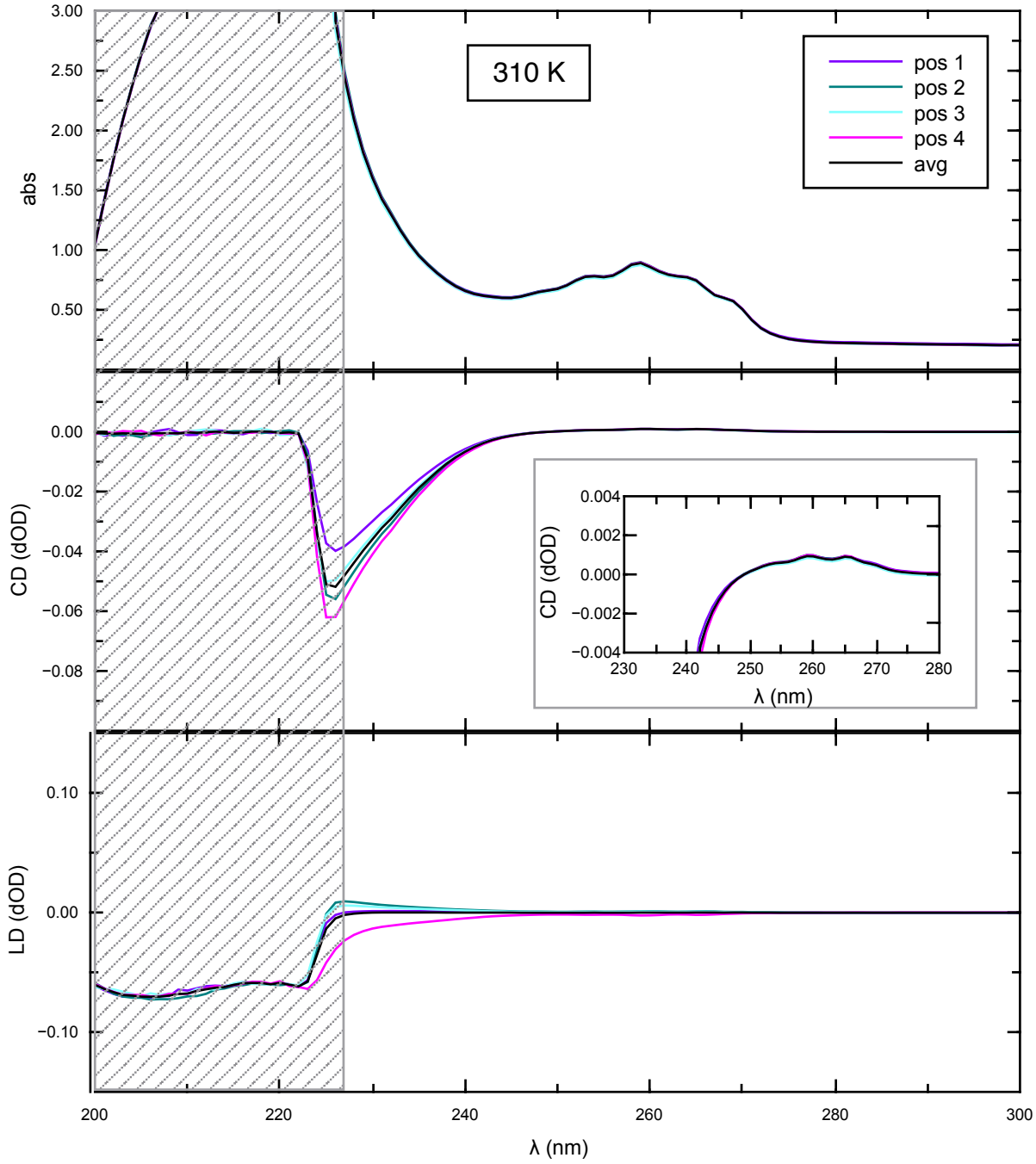

Figure S-17: Absorbance (top), CD (middle) and LD (bottom) spectra of LLC (PBLA-α-*d*)$_{50\%}$-co-PPLA$_{50\%}$ solution inside a parallelly aligned magnetic field with respect to the measurement beam at 310 K.

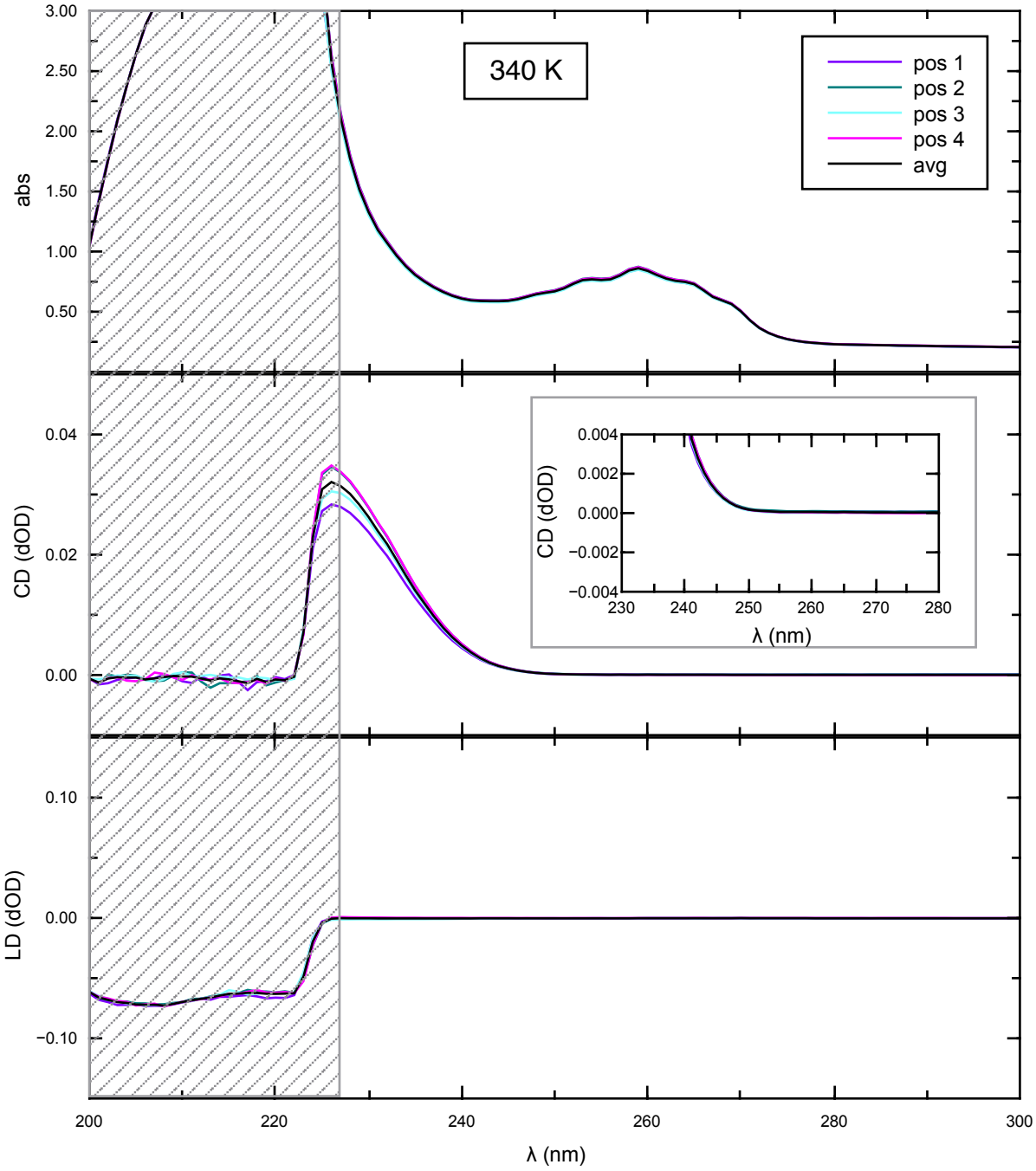

Figure S-18: Absorbance (top), CD (middle) and LD (bottom) spectra of LLC (PBLA-α-*d*)$_{50\%}$-co-PPLA$_{50\%}$ solution inside a parallelly aligned magnetic field with respect to the measurement beam at 340 K.

LLC (PBLA-α-*d*)$_{50\%}$-*co*-PPLA$_{50\%}$ Solution Inside Magnetic Field Perpendicular to the Measurement Beam

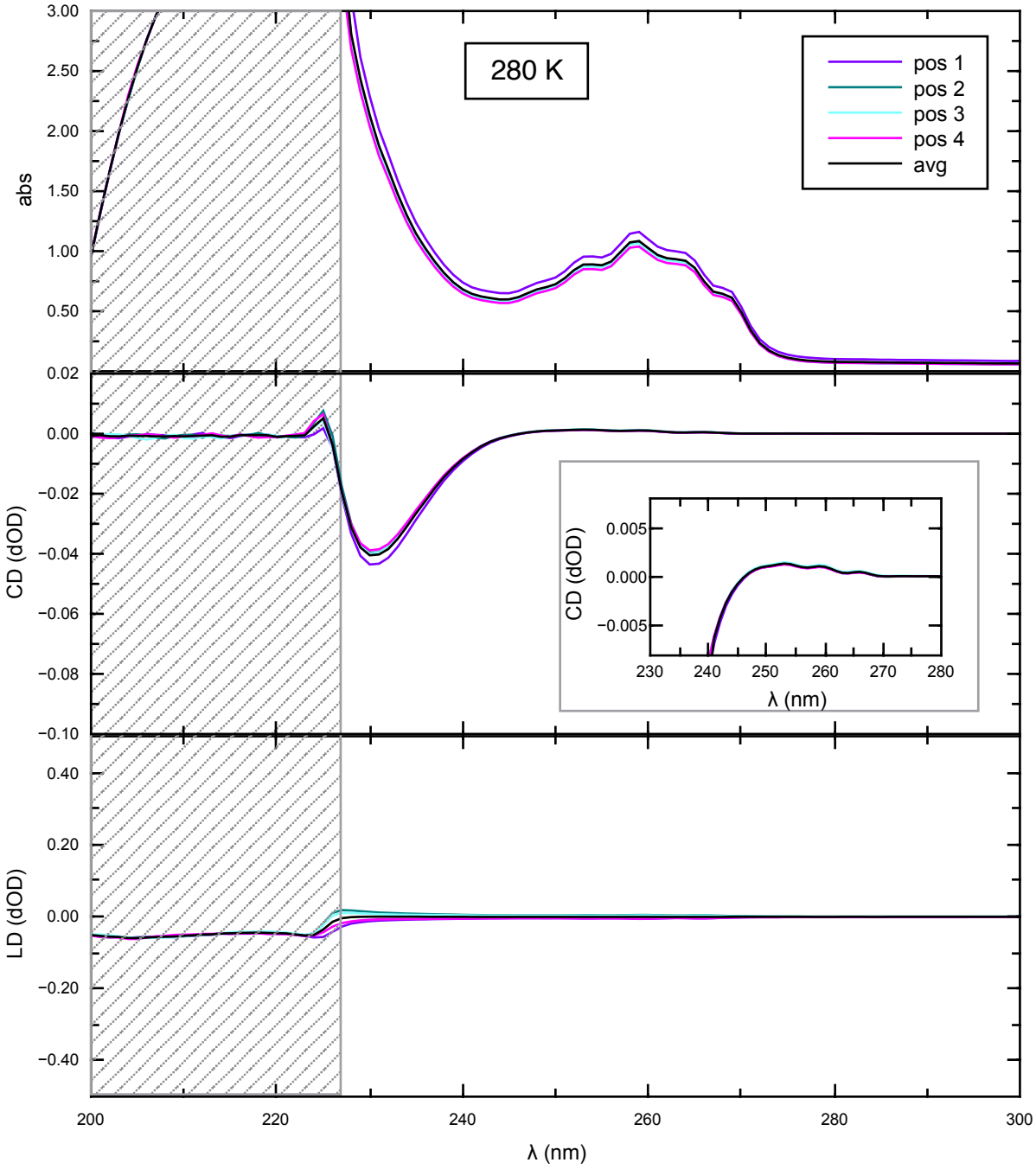

Figure S-19: Absorbance (top), CD (middle) and LD (bottom) spectra of LLC (PBLA-α-*d*)$_{50\%}$-co-PPLA$_{50\%}$ solution inside a perpendicularly aligned magnetic field with respect to the measurement beam at 280 K.

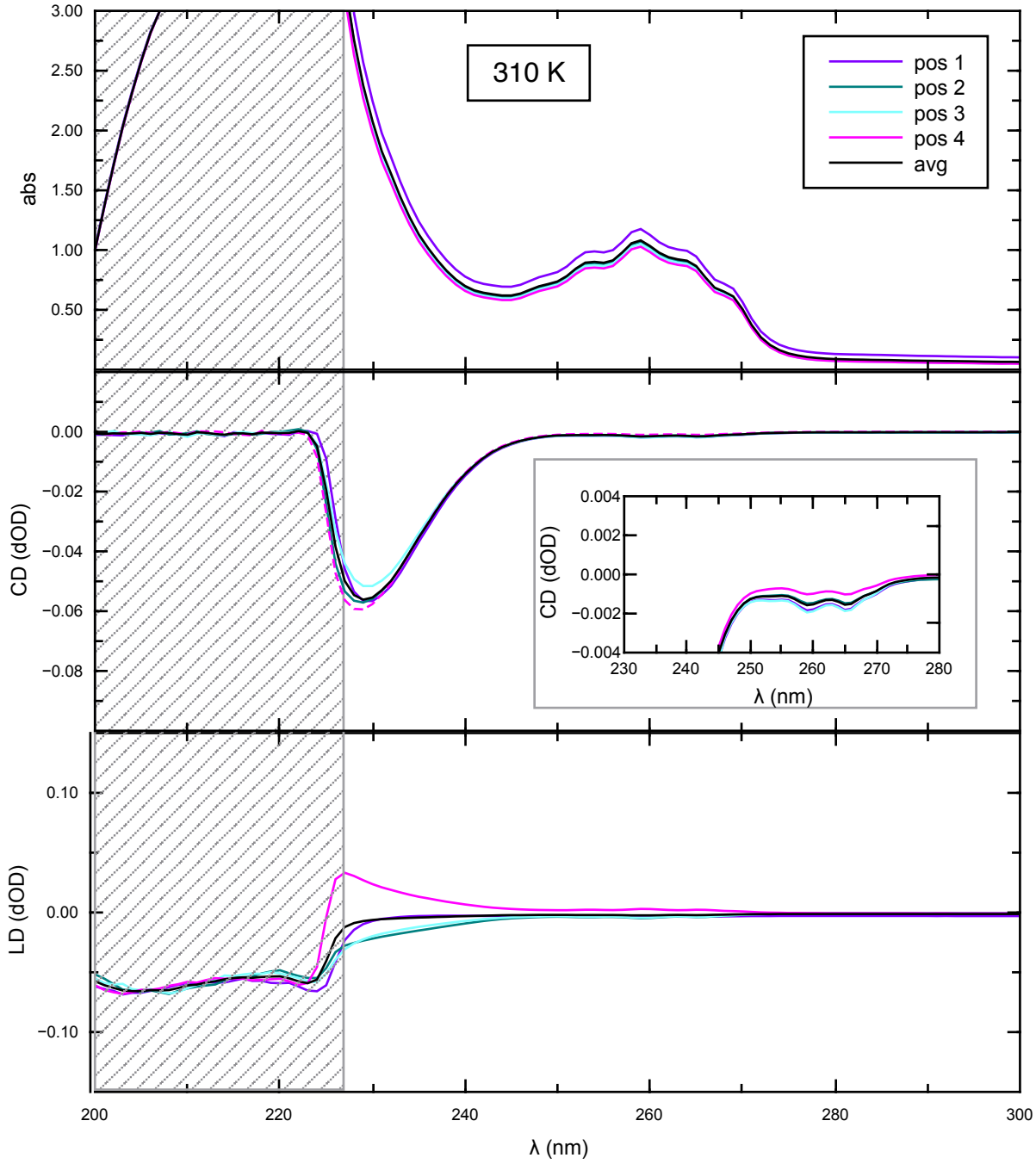

Figure S-20: Absorbance (top), CD (middle) and LD (bottom) spectra of LLC (PBLA-α-*d*)$_{50\%}$-co-PPLA$_{50\%}$ solution inside a perpendicularly aligned magnetic field with respect to the measurement beam at 310 K.

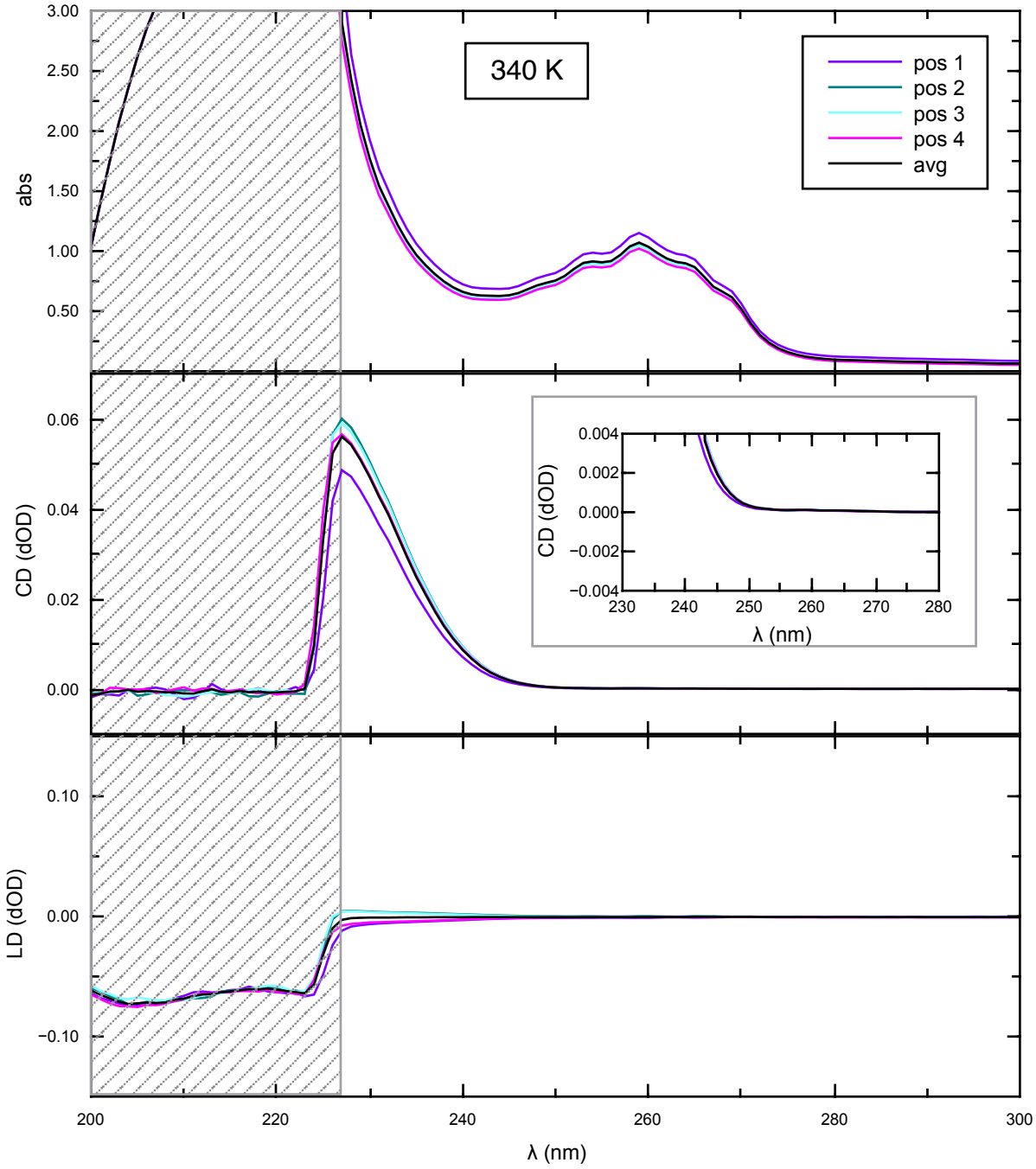

Figure S-21: Absorbance (top), CD (middle) and LD (bottom) spectra of LLC (PBLA-α-*d*)$_{50\%}$-co-PPLA$_{50\%}$ solution inside a perpendicularly aligned magnetic field with respect to the measurement beam at 340 K.

AO in LLC (PBLA-α-*d*)$_{50\%}$-*co*-PPLA$_{50\%}$ Solution Inside Magnetic Field Parallel to the Measurement Beam

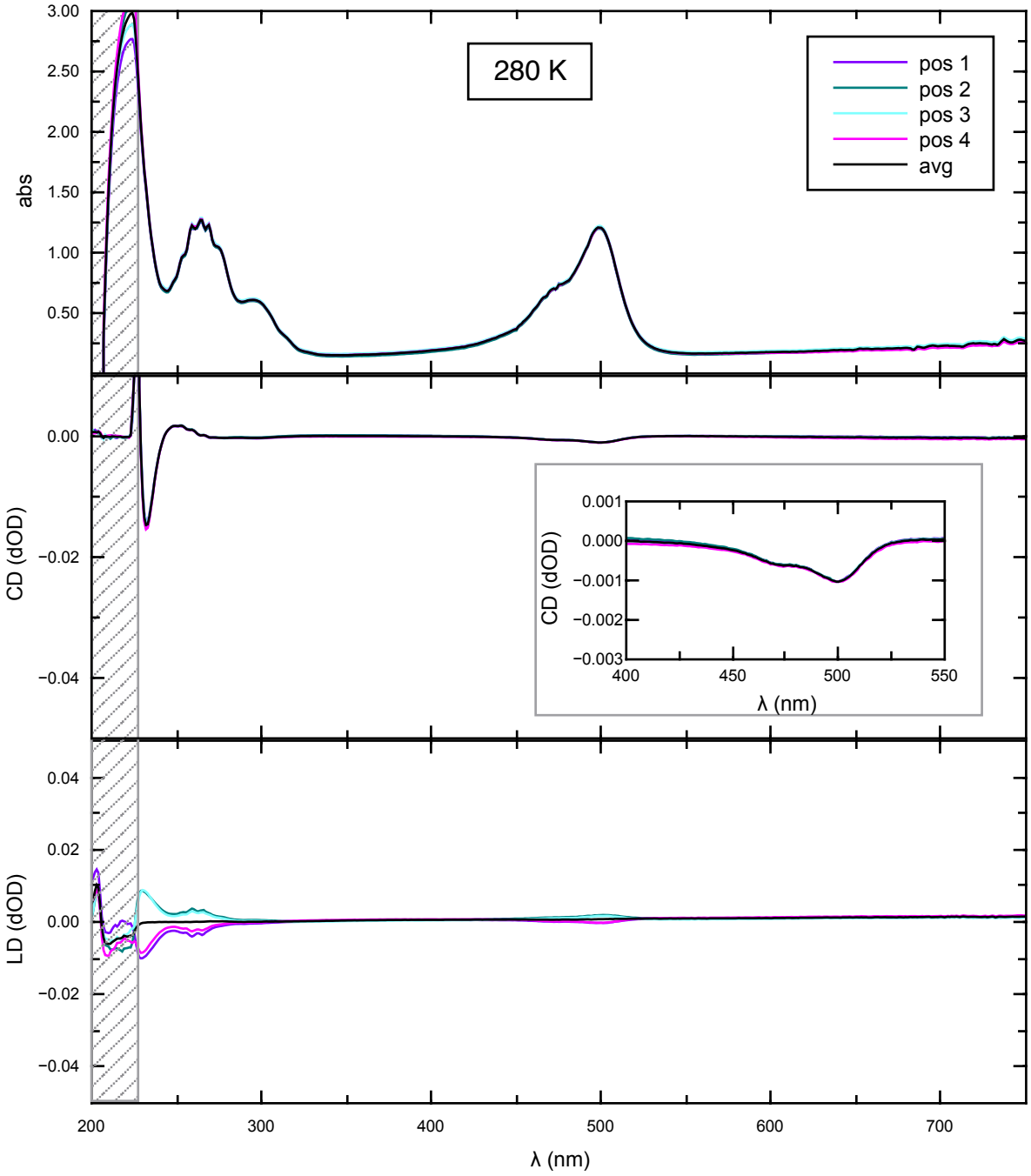

Figure S-22: Absorbance (top), CD (middle) and LD (bottom) spectra of AO in LLC (PBLA-α-*d*)$_{50\%}$-co-PPLA$_{50\%}$ solution inside a parallelly aligned magnetic field with respect to the measurement beam at 280 K.

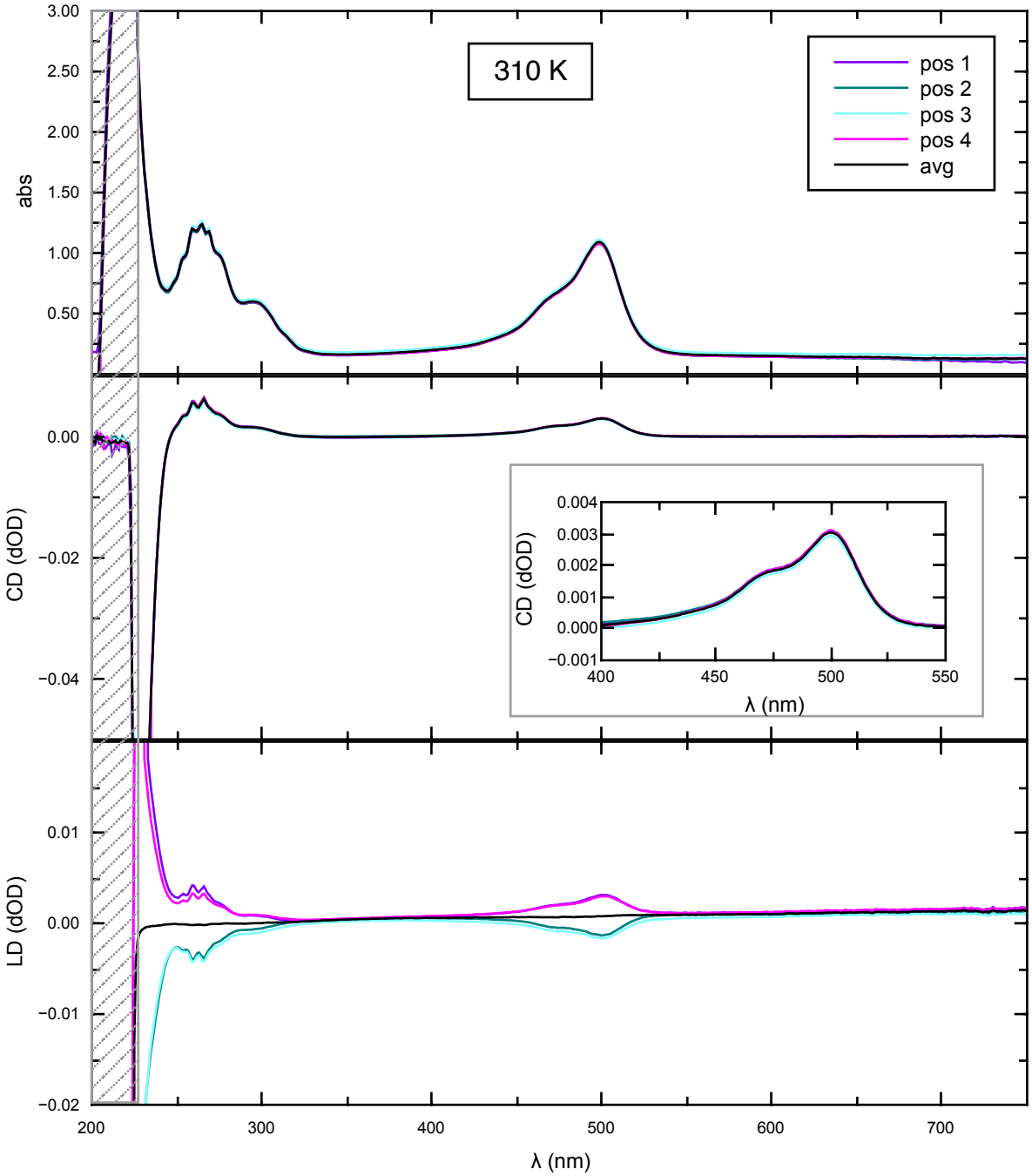

Figure S-23: Absorbance (top), CD (middle) and LD (bottom) spectra of AO in LLC (PBLA-α-*d*)$_{50\%}$-co-PPLA$_{50\%}$ solution inside a parallelly aligned magnetic field with respect to the measurement beam at 310 K.

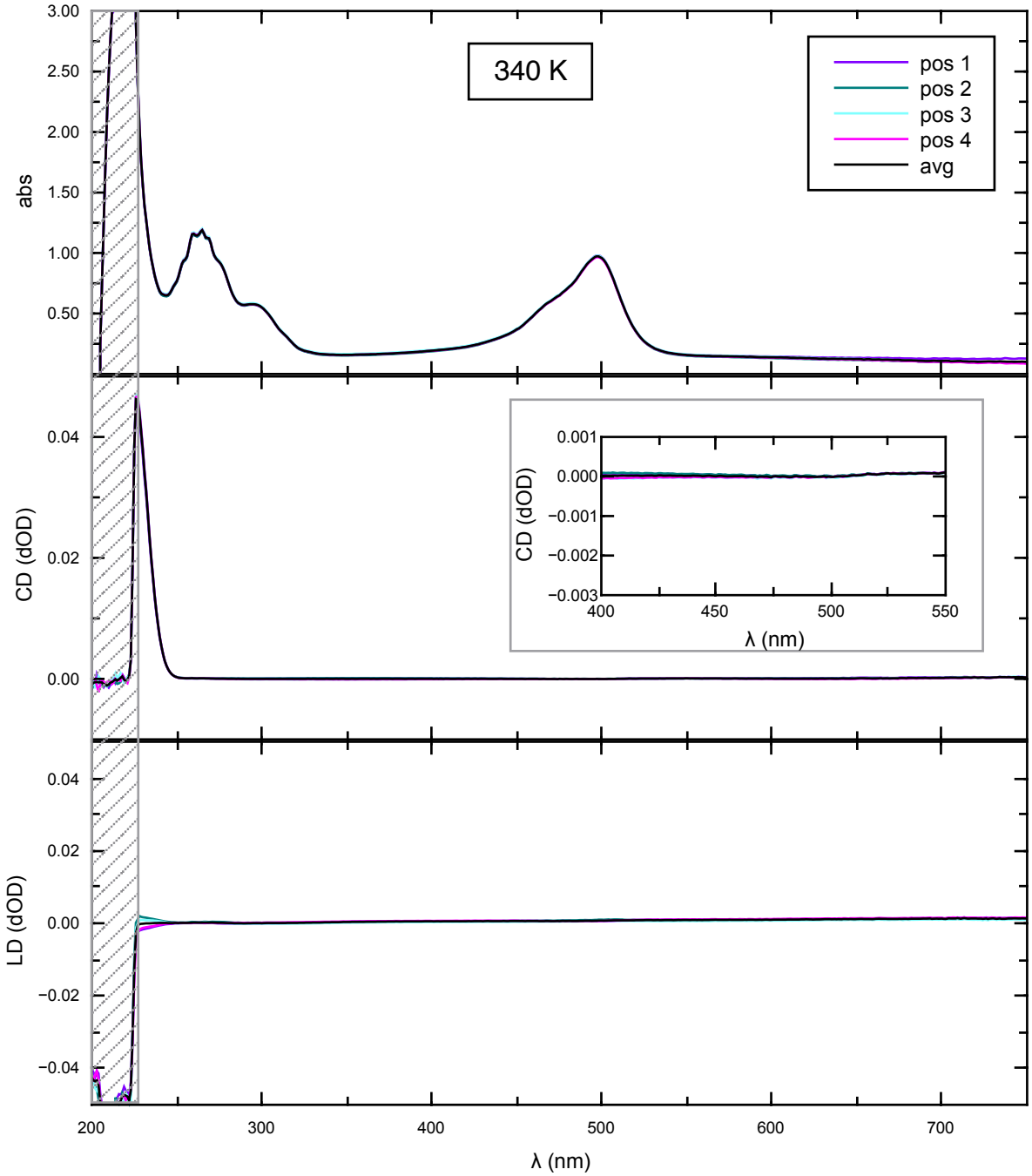

Figure S-24: Absorbance (top), CD (middle) and LD (bottom) spectra of AO in LLC (PBLA-α-*d*)$_{50\%}$-co-PPLA$_{50\%}$ solution inside a parallelly aligned magnetic field with respect to the measurement beam at 340 K.

AO in LLC (PBLA-α-*d*)$_{50\%}$-*co*-PPLA$_{50\%}$ Solution Inside Magnetic Field Perpendicular to the Measurement Beam

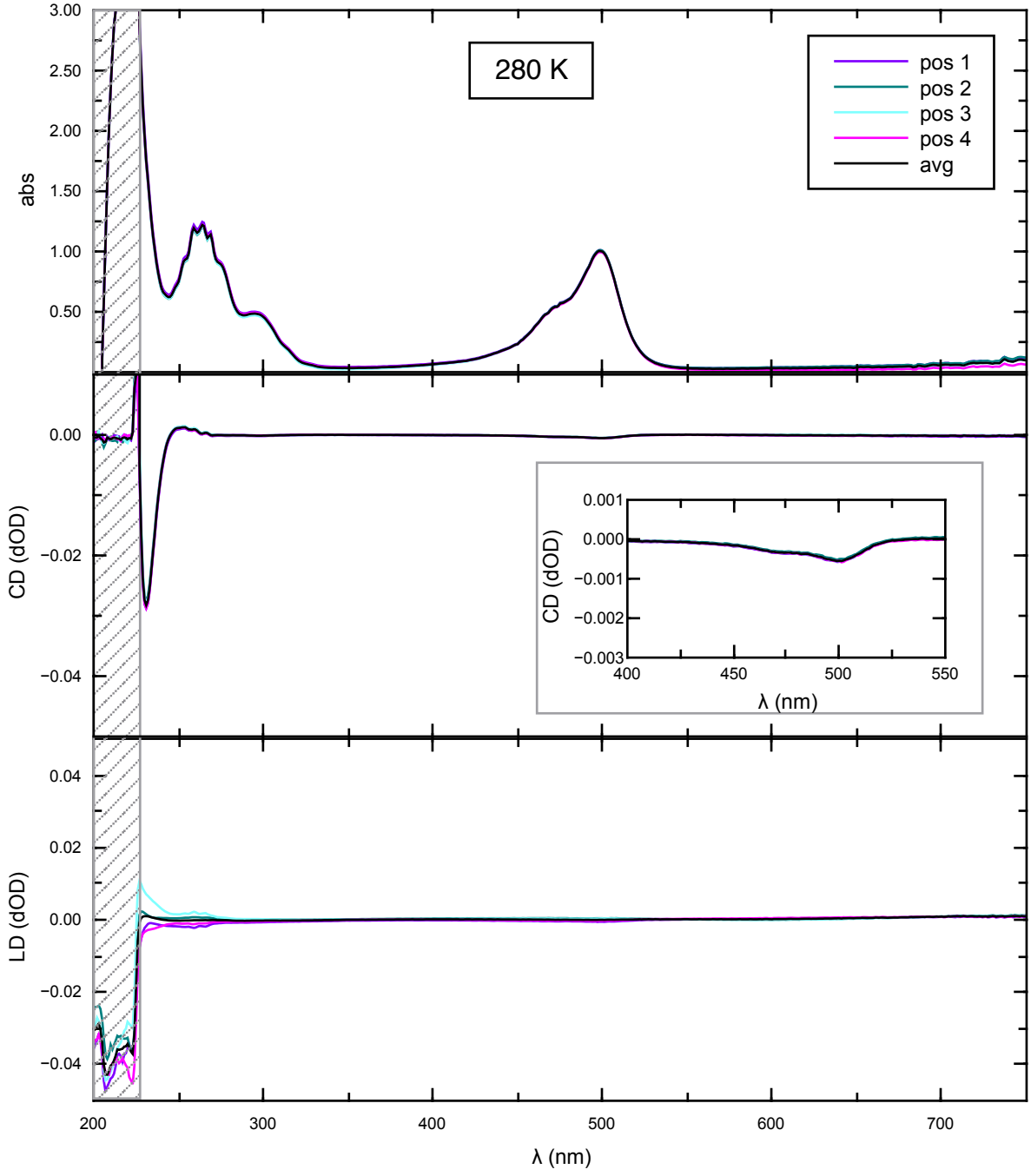

Figure S-25: Absorbance (top), CD (middle) and LD (bottom) spectra of AO in LLC (PBLA-α-*d*)$_{50\%}$-co-PPLA$_{50\%}$ solution inside a perpendicularly aligned magnetic field with respect to the measurement beam at 280 K.

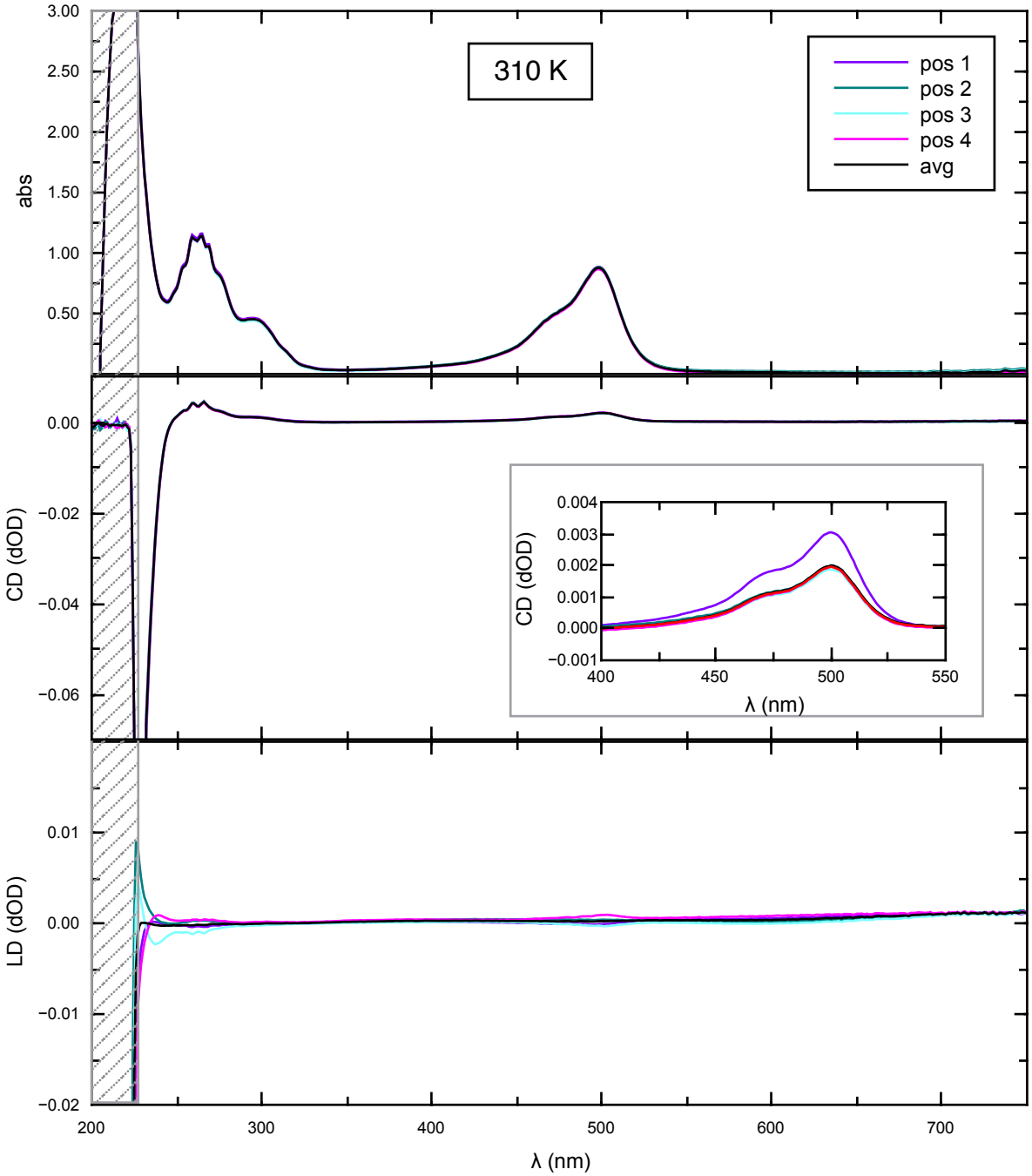

Figure S-26: Absorbance (top), CD (middle) and LD (bottom) spectra of AO in LLC (PBLA-α-*d*)$_{50\%}$-co-PPLA$_{50\%}$ solution inside a perpendicularly aligned magnetic field with respect to the measurement beam at 310 K.

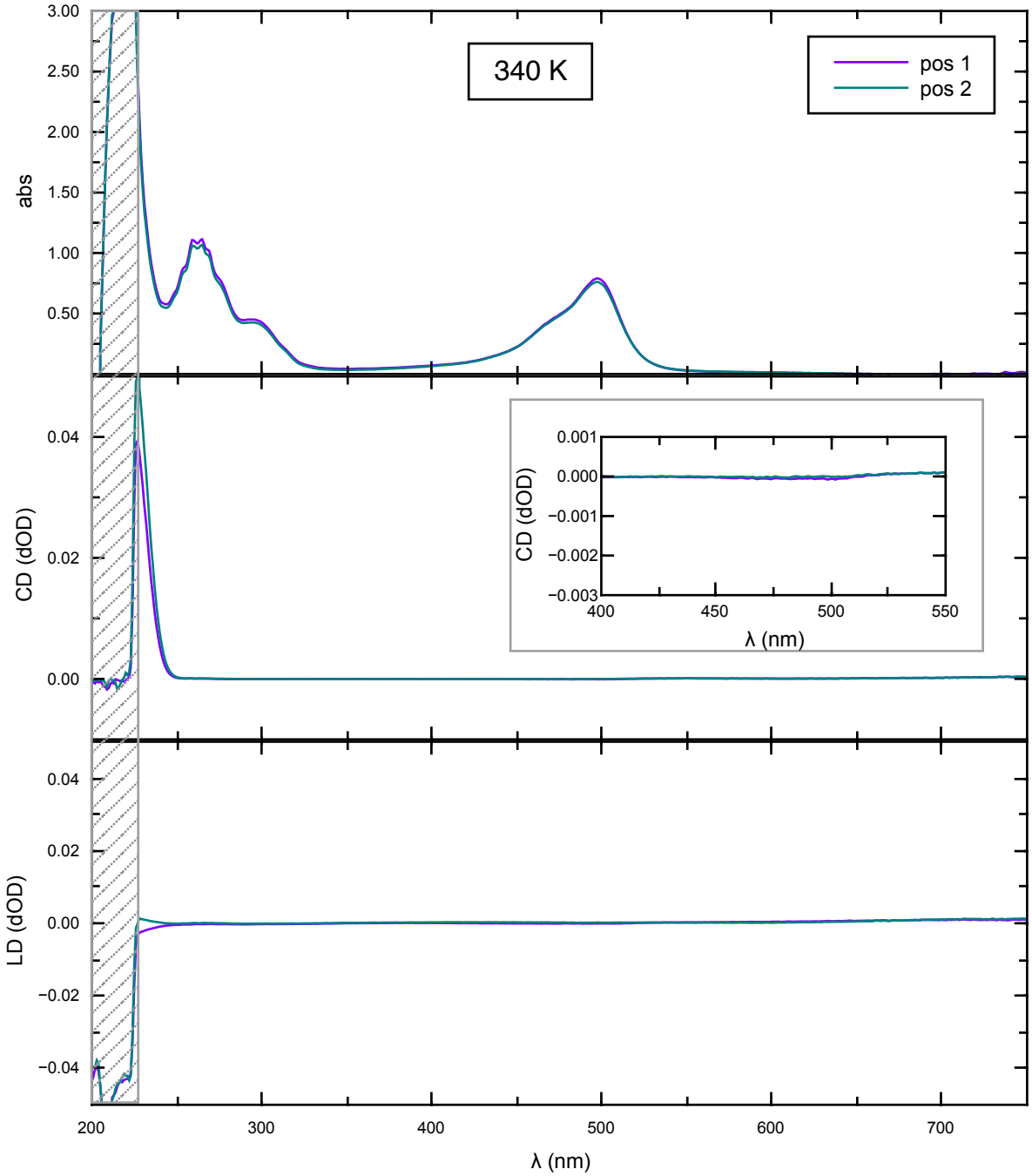

Figure S-27: Absorbance (top), CD (middle) and LD (bottom) spectra of AO in LLC (PBLA-α-*d*)$_{50\%}$-co-PPLA$_{50\%}$ solution inside a perpendicularly aligned magnetic field with respect to the measurement beam at 340 K.

Disodium Cromoglycate

Disodium cromoglycate (DSCG) is a known achiral compound, which is capable of forming LLC phases in water and has found its usage as alignment medium in NMR spectroscopy.[2,3] The absence of chirality and the ability to form LLC phases in water seemed to make DSCG LLC phases an ideal system for the proof of concept. Especially since a strong apparent CD of DSCG is shown[4] which we believed is based solely on anisotropic artefacts.

An LLC phase (14 %(w/w in H_2O) and an isotropic solution (1 %(w/w) in H_2O) of DSCG were prepared (procedure identical to the preparation of polymer LLC phases, apart from using different solvent / concentration and equilibration over night at 293 K). As expected, no CD and LD were measured for the isotropic solution (see Figure S-28). For the DSCG LLC phase a strong CD and LD were measured, the LD sometimes even exceeded the limit of the detector (1 dOD). But to our surprise the averaging of the four individual spectra did not result in a cancellation of CD. It does not even change sign upon rotation and cancellation of LD was not perfect either (see Figure S-29). We, therefore, repeated the preparation of the sample and its measurement twice (samples #2 and #3) and obtained different spectra every time. For sample #2 different signs of CD and LD were obtained upon rotation and averaging led to decent cancellation of both, CD and LD (see Figure S-30). Furthermore, although having the same concentration the optical density of sample #2 is reduced compared to sample #1 and no cut-off wavelength was observed. For sample #3, the apparent CD was positive at all orientations of the sample (in contrast to the negative CD observed for sample #1) and, consequently, averaging did not lead to cancellation of CD (see Figure S-31). Similar to sample #1, the cancellation of LD upon averaging was not perfect.

DSCG LLC phases are described to be formed by chiral subunits that are racemic in the absence of any chiral influence but a chiral LLC phase can be obtained by adding a chiral molecule into the LLC solution.[5] In theory such a chiral LLC solution could explain why averaging of the apparent CD does not lead to cancellation of the CD. Further, the observation of a negative and a positive CD, respectively (sample #1 *vs.* #3), could then be the influence of contaminations with different handedness. However, as chiral contaminations during the preparation of the DSCG sample were avoided as good as possible, this explanation seems not likely. When comparing the absorbance and CD spectra of sample #1, #2 and #3, different extrema are found. Furthermore, the extrema of CD and absorbance of the same sample do not match in every case. Aggregation is described for DSCG to result in different maxima in the absorbance spectra,[6] which would explain the differences in the absorbance spectra and suggests that aggregation is least present for sample #2. The aggregation could likely be induced by shearing, caused by the sample preparation[7] and is well-known to influence the CD spectra obtained.[8] Further evidence for aggregation, which is believed to happen on a prolonged timescale, is found by following the equilibration over time with CD spectroscopy (see Figures 32 and 33). Possibly, different forms or stages of aggregation were present in the samples that provide a source of chirality in the sample area, because the investigated sample area is too small to be regarded as racemic. Following this explanation, only in the absence of aggregation (or if the aggregates formed are still small) cancellation would be observed, which is likely the case for sample #2. However, even for sample #2 cancellation is not perfect, implying that either aggregates are already formed in sample #2 and / or that aggregation took place during spectra acquisition (which results in a change of CD etc. over time).

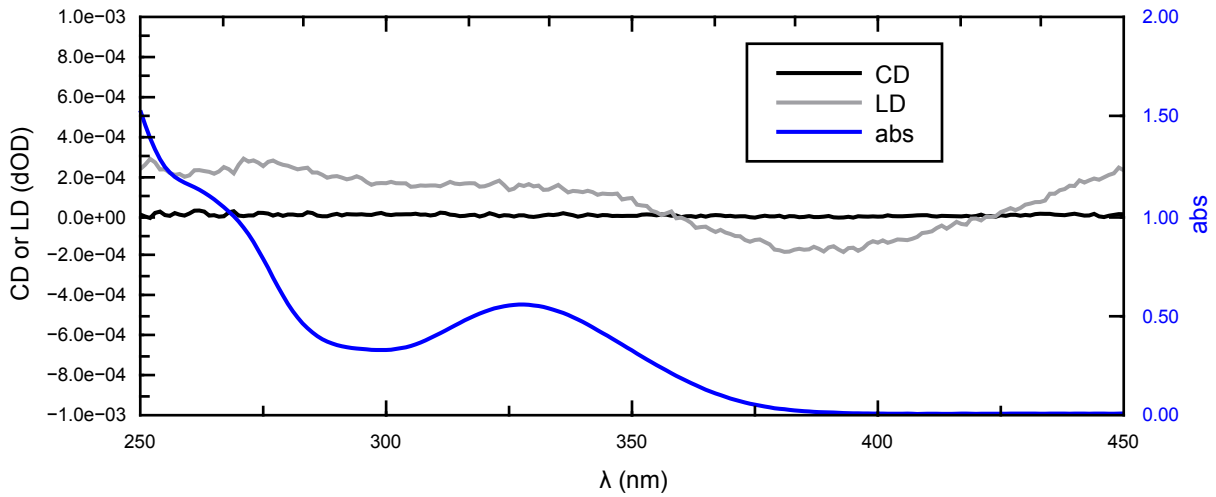

Figure S-28: Absorbance (blue), CD (black) and LD (grey) spectra of an isotropic DSCG solution (1 %(w/w) in H_2O).

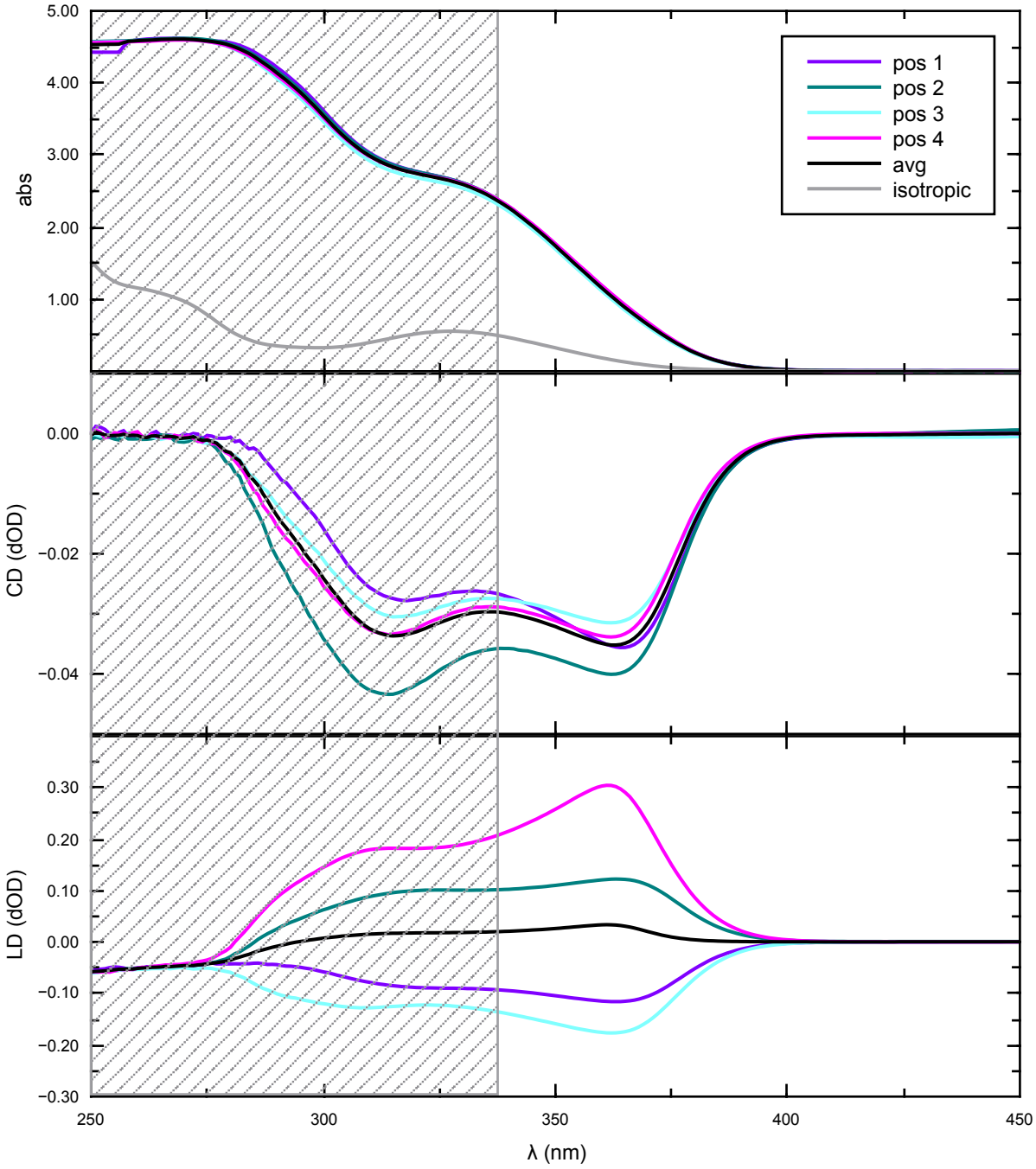

Figure S-29: Absorbance (top), CD (middle) and LD (bottom) spectra of LLC DSCG solution (sample #1) at 293 K.

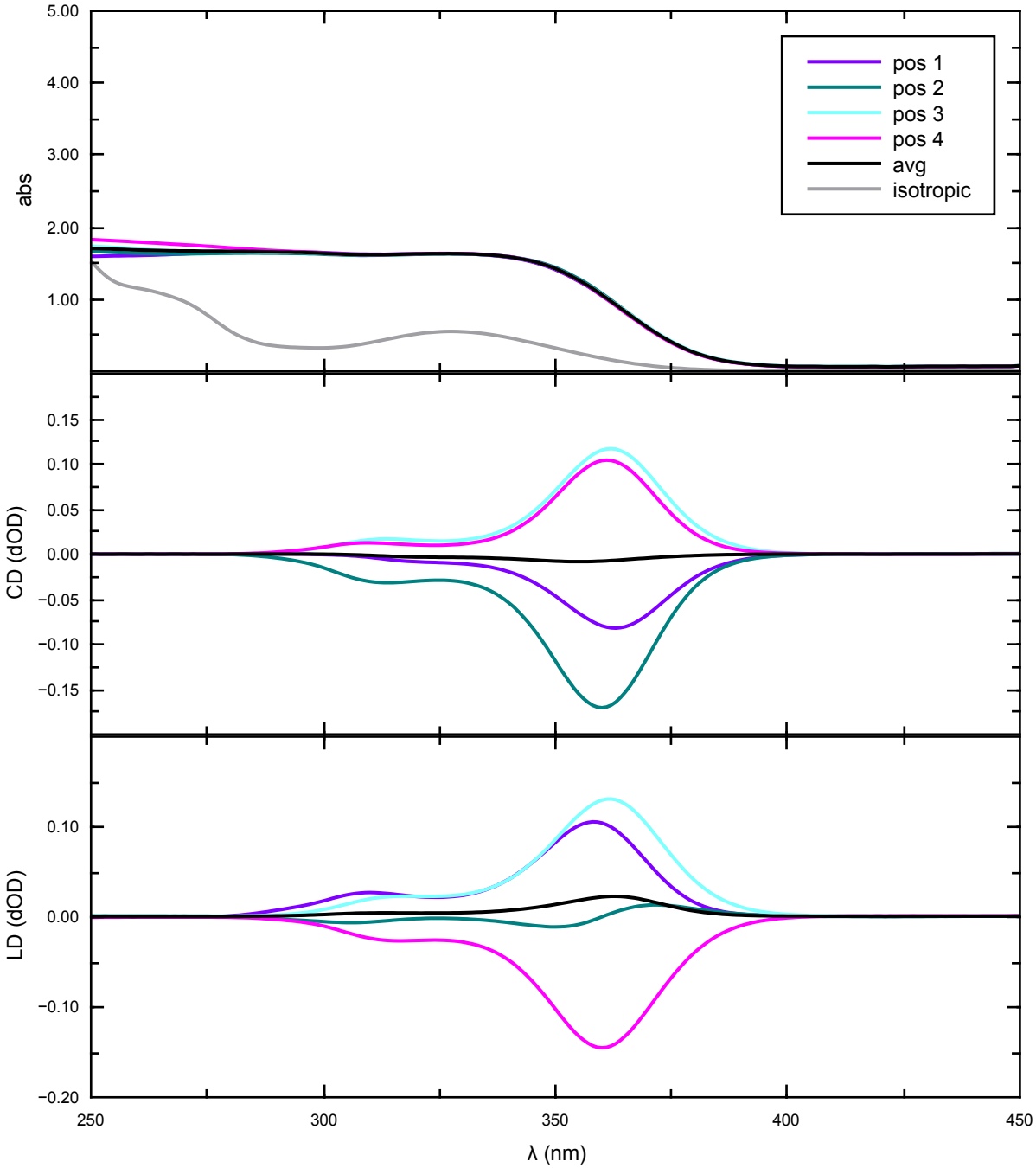

Figure S-30: Absorbance (top), CD (middle) and LD (bottom) spectra of LLC DSCG solution (sample #2) at 293 K.

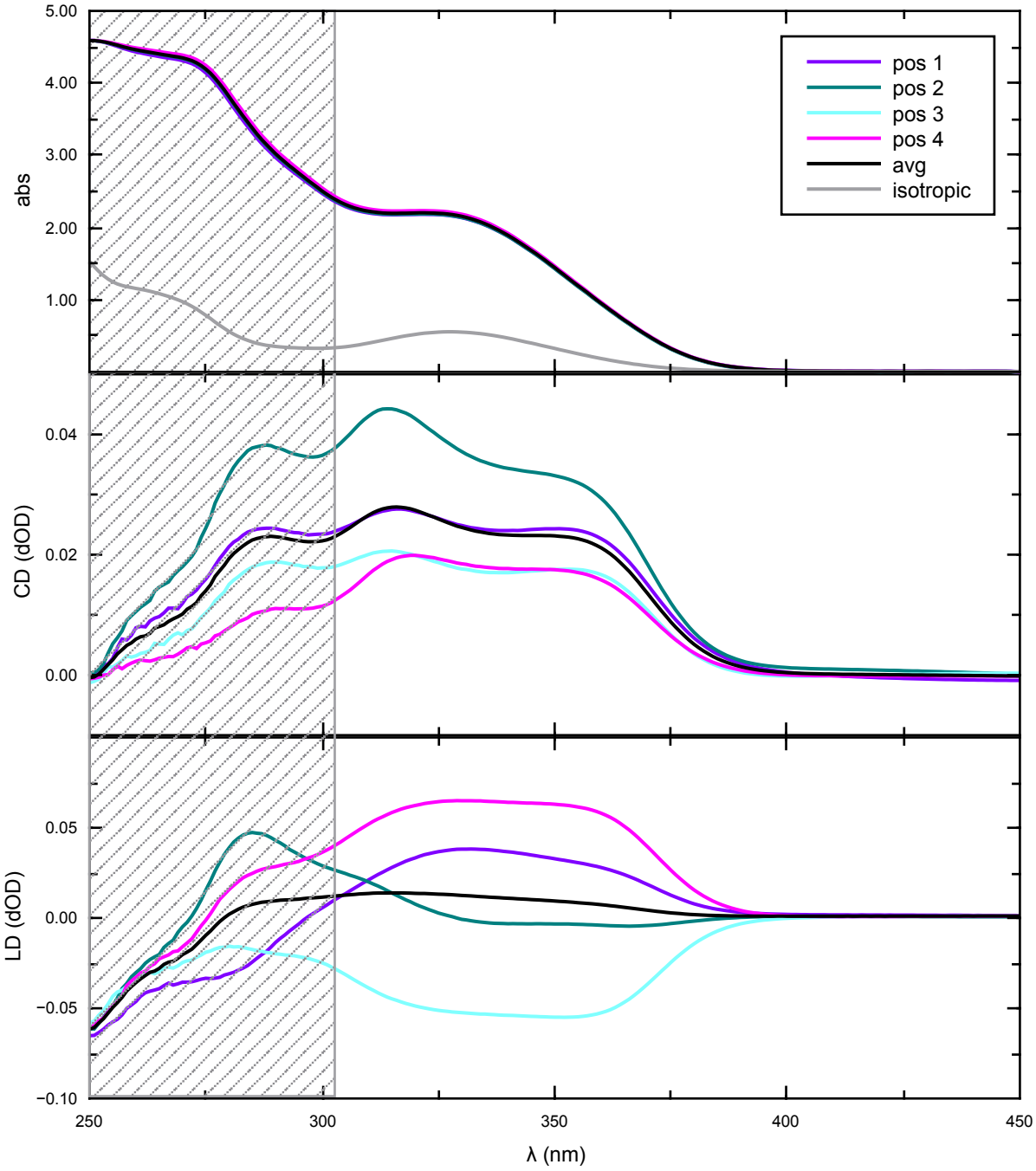

Figure S-31: Absorbance (top), CD (middle) and LD (bottom) spectra of LLC DSCG solution (sample #3) at 293 K.

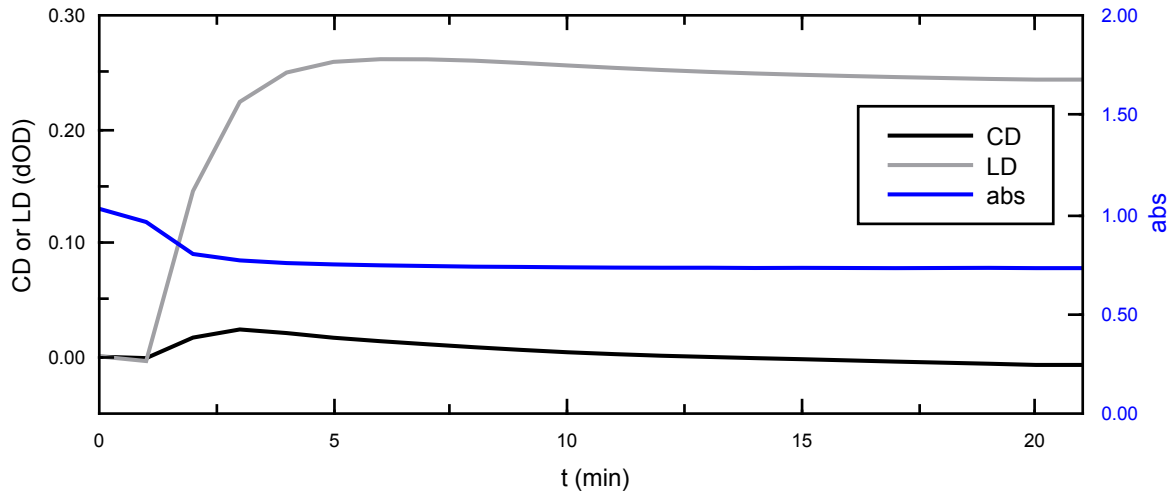

Figure S-32: Equilibration of 14 %(w/w) LLC DSCG solution (CD, LD and abs were measured at 365 nm). At time 0 the sample was equilibrated at 313 K inside the CD spectrometer. At this temperature the sample is isotropic and no CD and LD were observed. With start of the measurement the peltier element was set to 293 K. The temperature change of the peltier element and the cuvette (holder) takes a few minutes. At 293 K the sample becomes anisotropic again, which results in CD and LD (after ~ 2 min). As can be seen, the absorbance is only affected slightly by the temperature change and is constant over time after 3 min. On the other hand, the CD and LD change over time (including a sign change of CD), which is attributed to changes of the sample (e.g. alignment of the LLC structure or aggregation).

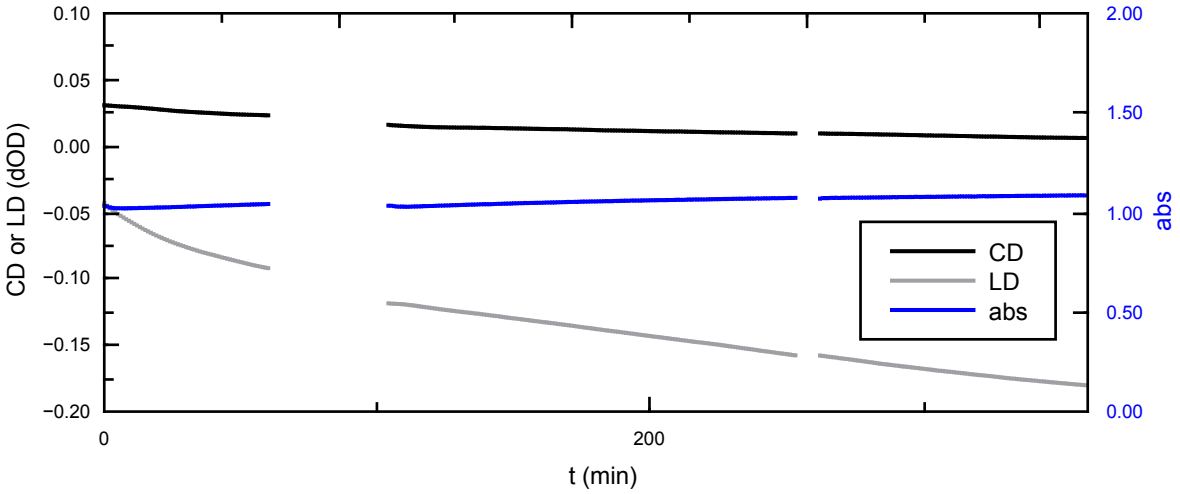

Figure S-33: Equilibration of LLC DSCG solution (CD, LD and abs were measured at 365 nm) directly after preparation of the sample. CD and LD do not reach a constant value over time indicating that equilibration of the sample is not finished. This behaviour can not be explained by a temperature change (contrary to the equilibration discussed in Figure S-32) and seems to have its origin in the sample preparation. A slightly modified LLC DSCG solution was investigated (9 %(w/w) DSCG in 0.3 %(w/w) aqueous brine), for which similar LLC structures at slightly lower concentrations are obtained compared to LLC DSCG solutions with pure H_2O as co-solvent.

References

1 D. C. Meeker, *Finite Element Method Magnetics*, 2018.

2 N. H. Hartshorne and G. D. Woodard, *Mol. Cryst. Liq. Cryst.*, 1973, **23**, 343–368.

3 E. Troche-Pesqueira, M.-M. Cid and A. Navarro-Vázquez, *Org. Biomol. Chem.*, 2014, **12**, 1957–1965.

4 F. Berride, E. Troche-Pesqueira, G. Feio, E. J. Cabrita, T. Sierra, A. Navarro-Vázquez and M. M. Cid, *Soft Matter*, 2017, **13**, 6810–6815.

5 C. Peng and O. D. Lavrentovich, *Soft Matter*, 2015, **11**, 7257–7263.

6 Y. A. Nastishin, H. Liu, T. Schneider, V. Nazarenko, R. Vasyuta, S. V. Shiyanovskii and O. D. Lavrentovich, *Phys. Rev. E*, 2005, **72**, 041711.

7 E. Iizuka, *Polym. J.*, 1973, **5**, 62–71.

8 A. von Weber, D. C. Hooper, M. Jakob, V. K. Valev, A. Kartouzian and U. Heiz, *ChemPhysChem*, 2019, **20**, 62–69.